SIXTEEN VALENCE-ELECTRON SPECIES CONTAINING BORON: STRUCTURAL DIVERSITY ABOUNDS

A Thesis Presented to the Faculty of the Graduate School

University of Missouri

In Partial Fulfillment

of the Requirements for the Degree

Master of Science

---

by

AARON K. CORUM

Dr. Carol A. Deakyne, Thesis Advisor

July 2005

The undersigned, appointed by the Dean of the Graduate School, have examined the thesis entitled.

SIXTEEN VALENCE-ELECTRON SPECIES: STRUCTURAL DIVERSITY ABOUNDS

Presented by Aaron Corum

A candidate for the degree of Master of Science

And hereby certify that in their opinion it is worthy of acceptance.

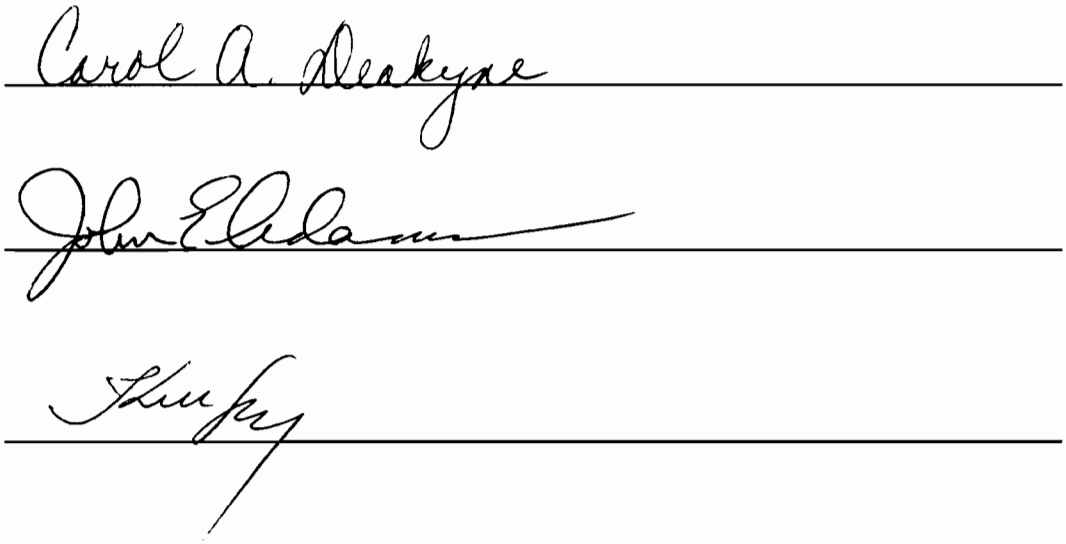

ACKNOWLEDGEMENTS

First I would like to thank my advisor, Dr. Carol A. Deakyne, for her patience and help on this work. I would also like to thank the members of my committee for their time and input. Tamas Szabo and Chad Magee, I would like to thank for their encouragement and input. Also, thanks to my family and friends for their encouragement to persevere. Lastly, I am eternally grateful to the One who has made all things possible.

ABSTRACT

[B, C, F, H_2] and [B, N, O, H_2] have been investigated at the MP2 and QCISD levels of computational theory with a valence double-zeta basis set augmented with polarization functions and diffuse functions (aug-cc-pVDZ). Both cyclic and acyclic connectivities have been examined for the singlet state. Geometries were optimized at both calculational levels and single-point energies were obtained at the QCISD(T) level with an expanded basis set (aug-cc-pVTZ). Chemical intuition suggests a ketene-like structure for each system, with the general form H_2XBY, where X = C or N and Y = F or O. The calculations yield a variety of possible structures for these species, including both cyclic and the expected acyclic, hydrogen-bonded and fluorine-bridged. Each isomeric form has at least one unique vibrational frequency of sufficient intensity to be identified through IR.

Eight minima have been located for [B, C, F, H_2] at both calculational levels: H_2CBF is the most stable, two structures contain a non-terminal fluorine, and an unconventional hydrogen bonded structure, a H_2 complex and a weakly bound heterodimer round out the interesting structures. Proton affinities were calculated using data from the $[B, C, F, H_3]^+$ system; carbon was found to be the most preferred protonation site, followed by boron and then fluorine. Five MP2 transition structures have been located for the [B, C, F, H_2] system, each connecting two of the MP2 minima. Barriers to the rearrangements between isomers have also been evaluated.

Thus far, 15 minima have been located for [B, N, O, H_2], also at both calculational levels. Among them are the analogous H_2NBO, also the most stable, two hydrogen bonded species—providing examples of both a conventional and an unconventional

hydrogen bond—and a cyclic system. All three possible connectivities for N, B and O have been examined. N-B-O was found to be the most stable connectivity, followed by N-O-B and O-N-B.

AIM and NBO analyses have been carried out to gain an understanding of the bonding in the various isomeric forms of [B, C, F, H_2] and [B, N, O, H_2]. These analyses suggest that B=C bonds form in the [B, C, F, H_2] system, whereas C=F and B=F bonds are unlikely to form. For isomers of [B, N, O, H_2], the analyses found evidence of the existence of B=O, B=N, and N=O bonds. Both systems have also been analyzed in terms of the Lewis acidity of BH, and BH affinities were calculated.

TABLE OF CONTENTS

LIST OF TABLES

TABLE OF FIGURES

Figure Page

INTRODUCTION

Molecules containing boron are often sensitive to heat, light, oxygen and water. Those containing nitrogen and hydrogen are particularly pyrophoric. Thus, small molecules containing boron are often very difficult to deal with in an experimental setting. However, with the use of matrix isolation, reactions with boron and small molecules such as CH_4, NH_3, C_2H_2, N_2, CO, and H_2 are possible.[1] These reactions have led to a number of basic small molecules that provide insight into the structure and bonding of boron-containing compounds.[1] In addition to these small molecules, researchers, namely Andrews et al., have studied the reaction of laser ablated boron with methylamines,[2] NO,[1] methyl halides,[3] methanol,[4] ethylene and ethane,[5] and HCN.[6] These reactions have also led to a number of novel structures.

Reacting boron with ethylene produces more than 12 novel BC_2H_x molecules.[5] Andrews et al. observed both cyclic aromatic and aliphatic products, which suggests that the reaction proceeds through both C==C addition and C—H insertion mechanisms.[5] Boron, in reactions with mono- and dimethylamine,[2] produced three new iminoboranes, CH_3BNH, CH_3NBH and CH_3BNCH_3, as well as the related isomer CH_2BNH_2. In reactions with CH_4[7,8] and NH_3,[9,10] Andrews et al. determined that the latter reactions yielded more product because the energy of the C-H bond in methane exceeds that of the N-H bond in ammonia. Analagous to the reaction of B with methylamine is boron's reaction with methanol. Three major new species come from this reaction, CH_3BO, CH_2BO, and CH_2BOH, all of which have B-O bonds, each with at least some multiple bond character caused by the oxygen atom lone pair coordinating with the empty boron p-orbital.[4]

For reactions of boron with methyl halides, Lanzisera and Andrews characterized H_2CBF and CHBF (two new products) as well as H_3CBCl, H_2CBCl, CHBCl, H_3CBBr, H_2CBBr, and CHBBr.[3] Compared with the other reactions of B, there are fewer possible reaction products. In the other reactions major products resulted from insertion between heavy atoms followed by H loss from the more electronegative heavy atom.[3] However, since in CH_3F the fluorine is terminal, this is not possible. Reaction of laser-ablated boron with HCN yields the previously unknown molecules BCN and BNC, as well as the products HBNC, HBCN, and cyclic HB(CN).[6]

In all of these reactions, Andrews and coworkers have used either DFT or ab initio computational methods to determine possible structures and to calculate the vibrational frequencies of the possible minima. These frequencies were compared to the observed IR frequencies from each experiment in order to verify the structure of the products.

One advantage of computational study versus experimental is that many reactive species that require extensive experimental setup (such as laser ablation of boron) or are dangerous to handle in significant quantities (such as explosives) can be safely examined computationally. Although these experimentalists have used computational methods to confirm and identify their potential reaction products, little work has been done on examining the entire potential energy surfaces of systems containing boron. This is not to say, however, that no computational work has been performed; only that much of what exists is more specific in nature. For instance, DiMare[11] has examined the importance of Lewis acid-base interactions in the proposed mechanism for the experimental gas-phase reactions of diborane with organic compounds.[12] Using ab initio calculations, he

optimized the minima and transition states of several carbonyl-borane adducts and concluded that Lewis acid-base chemistry was at the heart of carbonyl reductions by diborane, borane, and borane's adducts of DMS and THF.[11]

Rozas, et al.[13] have studied the ability of monohydride and monofluoride derivatives of boron, aluminum, nitrogen and phosphorus to form hydrogen bonds. They examined the energy gap between singlet and triplet configurations and calculated proton affinities of several atoms in each molecule, as well as the capacity of these atoms to act as hydrogen bond acceptors. One result of this analysis was that they were able to determine a relative order of the strength of the hydrogen bond with respect to the acceptor atom.[13] Schuurman et al.[14] used various correlation consistent basis sets to characterize the ground state potential energy surface of BH_5, a borane complex first isolated by Tague and Andrews.[15] The main focus of Schuurmann et al.[14] was to determine the precise dissociation energy of BH_5 into $BH_3 + H_2$. Ford[16] used ab initio methods to study the vibrational spectra of the van der Waals complexes of boron trifluoride with noble gases. He was able to confirm the directions of the wavenumber shifts for the BF_3 fragment that were observed experimentally and to establish a correlation between the polarizability of the noble gas and the distance between the two fragments. The boron-noble gas interatomic distance was found to be directly proportional to the polarizability of the noble gas.

Kiani and Hofmann[17] used density functional theory computations to develop a structural increment system for determining the structures of 11-vertex *nido*-boranes and carboranes (borane and carborane clusters). Malde et al.[18] studied the effects of replacement of nitrogen with boron in N-methylacetamide (NMA) to form

acetylmethyborane (BMA). They found that replacements such as this on peptides give greater proteolytic stability and more flexibility in some of the torsional angles, both of which are absent in naturally occurring peptides.[18] Jacquemin et al.[19] used ab initio computations to obtain large values of first hyperpolarizabilities in linear phosphorus-boron chains. Their results indicate that such chains have limited asymmetry (small charge separation and dipole moment) but possess very large delocalizability (large polarizability).[19]

Likewise, our group has long had an interest in improving our understanding of the structures and energetics of boron-containing compounds. Very little is known experimentally and computationally about the energetics of compounds containing boron, carbon, fluorine, and hydrogen. Prior computational work in the group includes a study of the isoelectronic complexes formed between borane(1) (BH) and CN^-, CO and CF^+, $[HB,C,N]^-$ [HB,C,O] and $[HB,C,F]^+$.[20] Placing these systems in brackets and separating the constituent atoms and fragments is meant to prevent any bias toward a particular arrangement of the atoms and fragments one might have, thus allowing for arrangements that may seem unusual, i.e. "improbable" at first glance. We use this notation throughout the rest of the work for the same reason. All possible connectivities were considered. Pappová et al.[20] worked under the principle that BH could operate as both a Lewis acid and a Lewis base. For this reason, they anticipated structural diversity in the minima obtained, which they found. Justification for this becomes apparent when one examines the Lewis structure for BH, :B—H. The lone pair on boron is available for use as a Lewis base, while the presence of only four valence electrons allows for its use as a Lewis acid. In fact, they also calculated the BH affinities for each of the systems, e.g. the

change in energy for the reaction $HBCF^+ \rightarrow BH + CF^+$. Pappová et al.[20] not only found a variety of isomers, from three membered rings to chains, they also found both singlet and triplet ground state minima.

The structural diversity of the above systems and a desire to explore more fully boron-containing species prompted an investigation of the cationic system, $[B, C, F, H_3]^+$,[21] a study closely related to the current work on $[B, C, F, H_2]$. In their study, Deakyne et al.[21] looked at all possible connectivities of boron, carbon, fluorine, and three hydrogens. They were able to locate ten minima on the singlet potential energy surface, again with an intriguing structural diversity. Deakyne et al.[21] used the Lewis acid-base nature of BH to compare and contrast the relative stabilities of some of the minima.

Chemical intuition suggests that $[CH_3BF]^+$ would be stable, as it is isoelectronically related to CH_3CN, $[CH_3CO]^+$ and $[CH_3N_2]^+$, all of which are stable molecules. In fact, this connectivity yields the most stable isomer for the cationic system. Accordingly, for the $[B, C, F, H_2]$ system chemical intuition implies that CH_2BF would be stable, as the isoelectronically related cumulenes, $H_2C=C=CH_2$ and $H_2C=C=O$, are known experimentally. The structural diversity found in our earlier work,[20,21] however, leads us to expect similar diversity in the types of structures for the neutral system.

Proceeding directly from the cation to the neutral system $[B, C, F, H_2]$ also allows the calculation of proton affinities for some of the structures in the neutral system. The large number of papers devoted to proton affinities produced each year gives an indication of the usefulness and importance of this thermodynamic quantity. Proton affinities (PAs) are directly associated with basicity,[22] as the basicity of the proton

acceptor determines how well that base takes on a proton. Gas-phase PAs can be used to identify structural effects on inherent molecular basicities. PAs are also of interest due to the role of the proton-transfer reaction in organic chemistry and biochemistry. Computational studies of proton affinities are especially useful because absolute magnitudes of the proton affinity are obtained.

The proton affinity corresponds to the negative of the standard enthalpy change for the reaction: $H^+ + B^{n-1} \leftrightarrow HB^n$, where n is typically +1 or 0.[22] It is the energy needed to remove H^+ from a molecule. The proton affinities of [B, C, F, H_2] are found by taking the difference between the calculated enthalpy of the protonated cation and the calculated enthalpy of the neutral species. From these calculations, we are able to ascertain the relative proton affinities of the B, C, and F atoms in these molecules. Rozas et al.[13] have also examined the relative PAs of C, B, and F and used their data to predict the abilities of certain molecules to act as hydrogen bond acceptors.

The results from [B, C, F, H_2] led us to the isoelectronic [B, N, O, H_2] system. We wanted to see if replacing the CF group with a NO group would increase the number and type of stable, unique structures. Nitrogen and oxygen tend to be 3-coordinate or 2-coordinate, rather than 4-coordinate or singly coordinate. So our hope was to see a larger number of minima as well as more unique structures by substituting the CF group with the NO group.

CALCULATIONAL DETAILS

Ab initio molecular orbital calculations were performed with use of the Gaussian 98[23] and 03[24] suites of programs. The minima on the singlet potential energy surfaces (PES) of [B, C, F, H_2] and [B, N, O, H_2] were determined using both Møller-Plesset

second-order perturbation, MP2,[25,26] calculations and quadratic configuration interaction, QCISD,[27] calculations with the aug-cc-pVDZ basis set.[28,29] Tight convergence criteria were utilized to optimize structures fully, and computed energies were then improved by performing single-point QCISD(T)/aug-cc-pVTZ calculations. Equilibrium structures were characterized by harmonic vibrational frequency calculations at the MP2/aug-cc-pVDZ and QCISD/aug-cc-pVDZ levels. From this point we will use MP2 to signify MP2/aug-cc-pVDZ and QCISD to signify QCISD/aug-cc-pVDZ; QCISD(T)//MP2 and QCISD(T)//QCISD will be used as substitutions for the QCISD(T)/aug-cc-pVTZ/ /MP2/aug-cc-pVDZ and QCISD(T)/aug-cc-pVTZ//QCISD/aug-cc-pVDZ single point calculations, respectively. We chose these computational levels and basis sets to remain consistent with our earlier work on the cationic system $[B, C, F, H_3]^+$. At the time, analytical frequencies could not be evaluated at the CCSD level, and so the slightly less expensive—less time-consuming—QCISD level was used.

For the higher-energy $[B, C, F, H_2]$ structures, we had some concern that restricted HF calculations were not appropriate and that an unrestricted HF wavefunction would actually prove to be lower in energy. Thus, for all but the two lowest energy structures, we also performed unrestricted MP2 (UMP2) and QCISD (UQCISD) calculations to compare the energies with the default restricted calculations. Also for the $[B, C, F, H_2]$ system, Quadratic Synchronous Transit, QSTN,[30,31] and Intrinsic Reaction Coordinate, IRC,[32,33] calculations were performed. QST2 calculations give an initial guess for a transition state by averaging the geometries of two minima. IRC calculations verify which minima each possible transition state connects. Transition states connecting the MP2/aug-cc-pVDZ minima were located. The transition structures were also

characterized by harmonic vibrational frequency calculations at the MP2/aug-cc-pVDZ level.

Correlation consistent basis sets, such as aug-cc-pVXZ where X=D, T, Q, etc., have been developed to retrieve the correlation energy of the valence electrons. These basis sets are designed to include simultaneously functions that contribute similar amounts of correlation energy at the same stage, regardless of the function type.[34] Errors are consistently reduced for each step up in quality; consequently the sequence of correlation consistent basis sets converges toward the basis set limit.

Electron correlation tells us how one electron affects and is affected by all of the other electrons in the molecular orbitals. The electron correlation energy is the difference between the HF energy and the lowest possible energy in a given basis set. The HF method overestimates the electron-electron repulsion because it fails to keep the electrons sufficiently far apart.[35] The three main methods for calculating electron correlation are Configuration Interaction (CI), Many Body Perturbation Theory or Møller Plesset n^{th} order perturbation theory (MBPT or MPn), and Coupled Cluster theory (CC).[36]

QCISD and CCSD are two of the truncated methods that have been developed to approach an exact solution to the Schrödinger equation. QCISD is derived from Configuration Interaction theory, which calculates all of the possible occupation schemes for all of the electrons, and thus, with a large enough basis set, provides an exact solution to the non-relativistic, time-independent Schrödinger equation, with the Born-Oppenheimer approximation. However, full CI calculations require far too much time for most systems of chemical interest. And so efforts to truncate the full CI to the singly, doubly, and triply excited determinants gave rise to CISD and CISDT. The coupled-

cluster theory developed by Cizek[37] adds all types of corrections to the reference wavefunction to infinite order.[38] In the truncated coupled cluster method CCSD, all singly and doubly excited determinants are generated. Closely related to CCSD, QCISD was originally developed as a way to correct for size-consistency errors in CISD.[38] QCISD(T) calculates the singles and doubles contributions directly, but uses perturbation theory to approximate the triples contribution. While neither CCSD nor QCISD are variational, this is generally not an issue since the underestimation of the correlation energy resulting from incomplete basis sets predominates.

NBO[39] and AIM[40] analyses were also performed on each of the minima in both the CF and the NO systems. These programs, included in the Gaussian 98 and 03 suites,[23,24] both provide information on bonding. NBO analysis[41-47] considers deviations in the molecular electron density from the best Lewis structure. It also associates the underlying localized orbitals with concepts such as hybrid orbitals, steric repulsion, resonance, and charge transfer, which are familiar to chemists. AIM theory[40] looks at variations in the electron density at various positions in the molecule. With AIM one can determine any quantum mechanical property of an atom as well as locate critical points in the electron density that indicate the existence of a bond between atoms. In attempting to bridge quantum mechanics and chemistry, AIM theory presents an uncomplicated, rigorous, functional, and powerful definition for two of the most basic components of chemistry: the atom and the bond.[48]

The interaction energies reported in this paper are all upper bounds because they have not been corrected for basis set superposition error (BSSE). BSSE is the spurious lowering of the energy of a complex compared to the energies of its constituent fragments

resulting from the greater flexibility of the basis set of the complex. We attempted to correct for BSSE using the Counterpoise method,[49] but the calculations were unsuccessful. Furthermore, the interaction energies reported in the literature,[50] with which these interaction energies will be compared, were not corrected for BSSE.

RESULTS AND ANALYSIS OF RESULTS

A. [B, C, F, H_2]

1. Structures

Minima. For [B, C, F, H_2], 38 cyclic, linear, bent or hydrogen-bonded arrangements of these five atoms were examined, for some of which different point groups were explored. Of the 38, only 9 connectivities yielded a MP2 equilibrium structure, and only 8 of those gave a corresponding QCISD structure. The eight QCISD isomers and the ninth MP2 isomer are illustrated in Figure 1 and are numbered in order of decreasing stability, with **1** being the most stable and **8** being the least. Note that we have only included those structures found at both levels of calculation in the numbering scheme. CH_2BF **1** is the configuration expected on the basis of our chemical intuition; as mentioned above, it is isoelectronically related to the cumulenes H_2CCCH_2 and H_2CCO. Combination of borane (1) with FCH yields isomer **2** FC(H)BH. A hydrogen-bonded species, HCH···FB **4**, lies about halfway down the order of relative energies. Also of interest are the methane-like $H_2C(B)F$ **3**, a 4-coordinate carbon structure, and C-B(H)F-H **6**, a carbene structure. Additional minima include the unbranched HC-B-FH **5** structure and the weak heterodimer HCF···BH **7**. Structure **8** is a van der Waals complex between the hydrogen molecule and triatomic FCB species, H_2···C(F)B. The ninth MP2 minimum rearranges to **8** at the QCISD level. Note that **9** is shown with its MP2 geometry while all

others are shown with their QCISD geometries. Also note the presence of a bridged fluorine atom in two (**5** and **6**) of these configurations. Bridged fluorines have also been found in other inorganic compounds[51,52] and in organic compounds.[53,54,55]

Table 1 gives the isomers' geometries, including bond lengths, bond angles, and dihedral angles. Geometries are usually similar between the two levels of calculation. The calculated bond distances tend to be slightly longer at the QCISD level. The calculated bond angles are equally divided as to which level gives smaller and which larger angles. In general, the C-H, B-H, F-H, C-B, C-F, and B-F bond lengths differed by no more than 0.008 Å between the two levels, and most differences were even smaller. The H···F hydrogen bond distance differs by 0.070 Å, and two C-B bond distances differ by 0.011 Å and 0.088 Å. The greatest difference in B-F bond lengths comes from those structures with a bridged fluorine. **5** and **6** give a difference of 0.037 Å and 0.084 Å, respectively. With the exception of isomer **4**, the MP2 and QCISD optimum bond angles vary by no more than 7° and most vary by less than 2°. The analogous difference for **4** is considerably larger at 11°.

There is one major exception to the geometric consistency between levels; HH···C(F)B **8** has a dramatically different orientation at the MP2 level than it does at the QCISD level. The dihedral angles for this isomer vary by 19° and 40°. As a point of contrast, the dihedral angles for **6** only vary by 3°. The geometric differences in **8,** and the inability to find a corresponding QCISD structure for **9** has led us to conclude that we cannot stop with MP2 optimizations. However, the relatively quick MP2 optimizations do provide excellent starting geometries for the more time-consuming QCISD calculations.

Comparing a particular bond type among the minima, we find that bond distances do vary from structure to structure. C-H bonds fall around 1.09 Å, except for the four-coordinate **3**, the hydrogen-bonded species **4**, and the heterodimer **7**. These all have slightly longer bonds at around 1.12 Å. There are three B-H bonds, two of which fall at around 1.18 Å in length and the third, in the heterodimer **7**, is again longer at 1.24 Å. The F-H bond lenghts all center around 0.94 Å. For C-B, bond lengths vary from 1.36 Å to 1.69 Å. Half of the C-F bonds lie around 1.34 Å and the other half around 1.40 Å in length. The longest B-F bond is about 2 Å long, in the carbene **6**, and the second longest B-F bond is about 1.6 Å long. The final two B-F bonds are shorter, falling around 1.3 Å.

Multiple Bond Character. Looking at the delocalized orbitals for each structure, we see evidence of C-B multiple bonding in four of the eight minima, but very little evidence of C-F multiple bonds. Figure 2 shows the orbital pictures for the mentioned π-bonding interactions. For the following discussion the heavy atoms are oriented in the XY plane. For CH_2BF **1**, the p_z atomic orbitals in the HOMO, MO 11 (Fig. 2A), have coefficients of 0.433 and 0.305 for carbon and 0.333 and 0.186 for boron. The relative similarities in the two sets of magnitudes for carbon and boron indicate a bonding π-interaction, and with no corresponding occupied anti-bonding π-orbital, it is likely that the CB bond in **1** is a double bond. The analysis for the B-F bond, however, is not as clear cut. While there is a suggestion of a π-interaction in MO 7 for boron and fluorine, the overlap between boron and carbon is much larger. There is a similar weak BF interaction in MO 8, with p_z coefficients of 0.639 for fluorine and 0.121 for boron. However, the π–bonding interactions are partially offset by the antibonding π–character of MO 10 for boron (0.0798) and fluorine (-0.08009). So, while there may be some

multiple bond character to the B-F bond, the back-bonding from F to B appears to be minimal. For **2**, F-CH-BH, we have the possibility of CB and, although less likely, CF multiple bonds. There does appear to be a weak π–interaction in MO 8 between fluorine (0.635 and 0.432) and carbon (0.139 and 0.054); however there is a stronger antibonding π–interaction (Fig. 2B) between C (-0.203 and -0.156) and F (0.413 and 0.301) in MO 11. In MO 11 we do see evidence for a C-B double bond with p_z coefficients on boron of 0.374 and 0.190 and on carbon of 0.413 and 0.301. CH_2FB **3**, does not have any multiple bond character, as expected for a tetrahedral carbon atom. For the hydrogen bonded HCH···FB **4** we might expect some multiple bond character between fluorine and boron, but the π–interaction is again weak. MO 7, which has p_z coefficients of 0.119 and 0.00767 on boron and 0.642 and 0.435 on fluorine, is essentially a fluorine lone pair. There is likewise little indication of B-F multiple bonding in HF-B-CH **5** (Fig. 2C) and the carbene **6** (Fig. 2D). In contrast, the HOMO for both of these molecules again has a strong attractive π–interaction between B and C. The carbon p_z coefficients are 0.423, 0.292 and 0.423, 0.321 for **5** and **6**, respectively. The corresponding boron coefficients are 0.369, 0.223 and 0.341, 0.179, respectively. Note the similarity in the magnitudes of the p_z atomic orbital coefficients for molecules 1, 2, 5 and 6 for which there is a strong π–overlap between boron and carbon.

The heterodimer **7**, shows a small C-F π–overlap in MO 7, though the orbital is comprised of mostly F character (C: 0.126 and 0.048; F: 0.635 and 0.438). In addition, the MOs for **7** indicate that there is at best a weak covalent interaction between the B-H and H-C-F fragments; in fact, the AIM analysis does not locate a bond critical point between B-F or B-C. Although there appears to be little covalent character to the

interaction between the two fragments, the C-F and B-H bond dipoles are aligned favorably for a dipole-dipole interaction. Thus **7** may be a weakly bound intermediate on a fragmentation pathway of one of the lower energy structures, possibly **2**. Structure **8** shows only a limited multiple bond interaction between boron and carbon in MO 11 with coefficients of 0.118 and 0.0487 for boron and 0.178 and 0.123 for carbon.

The lack of a bond critical point between B-F or B-C in **7** may be correct, or it may be due to known problems that AIM has with systems involving B-F and C-F bonds.[56] The AIM analysis did not complete for many of the [B, C, F, H_2] isomers and fragments. When it did, it often gave ridiculous charges and unrealistic bond orders. For instance, for the B-F fragment, the charges given for boron and fluorine are 4.56 and 8.80 respectively, while the AIM bond order given is an absurd -11.89. For the HCF fragment, the charges on each of the atoms are all positive; the C-F bond order given is -7.07. For **1**, all of the atoms have positive charges, the CB bond order is -40.37, and the BF and CH bond orders are around 6.

Transition States. Thus far we have located six transition structures, shown in Figure 3. Five of the six connect different minima; the labeling denotes which minima each transition structure connects. The first transition structure in the figure connects minima **1** and **2**. We have also found transition states for the conversion between **1** and **3**, **2** and **3**, **2** and **5**, and **3** and **4**. BH_2CF, **TS2-2**, is a transition state for proton switching in **2**. Originally we expected BH_2CF to be a minimum due to Andrews' and Lanzisera's results from their DFT calculations.[3] However, increasing the size of the basis set changes the BH_2CF connectivity from a minimum to a transition state, even at the DFT level.

As presented in Figure 3 the conversions between structures are all endothermic. These reactions appear to follow Hammond's Postulate[57] which says that if a reaction is endothermic, the transition state will resemble the product. Two of the transition states have structures similar to what is expected based on chemical intuition. Interconversion of CH_2BF **1** to $H_2C(B)F$ **3** involves transfer of the fluorine atom from boron to carbon. Transition state **TS1-3,** shown in Figure 3B, shows the fluorine moving across the C-B bond. Likewise, rearrangement of F-CH-BH **2** to form **3** involves transfer of a hydrogen to the carbon. Transition state **TS2-3** (Figure 3D) shows a hydrogen atom moving across the C-B bond. The other three transition states have more interesting features. Conversion from CH_2BF **1** to F-CH-BH **2** involves exchange of hydrogen and fluorine atoms. If one follows the reaction path from lower to higher energy, **TS1-2** (Figure 3A) is interesting in that the proton has completely transferred from the carbon to boron before the fluorine begins to move. Most simply, transformation of **2** to H-F-B-CH **5** could occur via insertion of the fluorine into the B-H bond. **TS2-5** (Figure 3E) is interesting because the hydrogen and the fluorine on the carbon move simultaneously with the hydrogen on the boron, rather than the fluorine merely inserting into the B-H bond. Finally the reaction H_2CFB **3** → $HCH^{\cdots}FB$ **4** necessitates the fragmentation of **3**, suggesting that **4** may be a weakly bound intermediate on the dissociation pathway of **3**. In **TS3-4** (Figure 3F), the new B-F bond has already formed and the CH_2 and BF fragments merely need to rotate in space to form the product isomer.

2. Energetics

Minima. QCISD(T)//QCISD total energies, enthalpies and free energies, are listed in Table 2. ZPE corrected energy values are also given. Stability tests of the

wavefunction revealed that most of the structures, excepting **1** and **2**, may favor open shell electronic configurations or may exist as lower energy triplets. However, optimizations of the structures using the unrestricted MP2 and QCISD computations show no significant difference in the energies of the minima as opposed to the restricted computations. So the energies reported are those using the restricted HF wavefunction. As this work evaluates the singlet potential energy surface, triplet calculations will be performed subsequently.

Energies relative to **1** are listed in Table 3. The difference in the QCISD(T)//QCISD total energies between the most stable structure, H_2C-B-F **1**, and the second most stable, F-CH-BH **2**, is about 250 kJ/mol. The difference between the most and least stable, the H-H···Y complex HH···C(F)B **8**, is about 760 kJ/mol.

Figure 4 shows a plot of the zero-point corrected energies E_0, for each of the four levels of calculation considered in this work, MP2, QCISD(T)//MP2, QCISD, and QCISD(T)//QCISD. It provides additional insight into why we cannot limit our search for minima to the MP2 level and why we carry out the single point calculations. The MP2 and QCISD energies do not follow the same trend, their ordering of **4** and **5** is reversed. While the two sets of single point energies overlap when structural differences are small, they diverge in the placement of **8**. Also, although the trend in the QCISD//QCISD relative energies is consistent with that of the QCISD(T)//QCISD energies, the magnitudes of the relative energies at the two levels differ by as much as 50 kJ/mol.

Figure 5 shows a comparison of the thermochemical data obtained with the QCISD(T)//QCISD calculations. In addition to E_0, the enthalpy H and free energy G at

298 K for each minimum is compared in the figure. Notice that the changes in free energy track the changes in enthalpy. For the most part, entropy does not appear to be a factor in determining the relative stabilities of these systems. Similar trends are seen for the QCISD(T)//MP2 calculations.

*Isomer **1** versus isomer **2**.* The relative energies of **1** and **2** can be understood qualitatively by comparing the Lewis acidity and basicity of their fragments. If we compare the Lewis acidity of B-F versus B-H, we would expect B-F to be a better Lewis acid (electron pair receptor) than B-H because of the electron withdrawing nature of fluorine. The NBO analyses of the B-F and B-H fragments support this expectation. For B-F, there is more boron character in the unoccupied σ*(B-F) orbital and a lower electron density in the unoccupied lone pair orbital on boron n*(B), compared to the corresponding orbitals for B-H. Thus B-F is a better Lewis acid than B-H. Likewise, we expect that H_2C is a better Lewis base than HCF, because fluorine will pull more electron density away from carbon than hydrogen will, making the carbon in HCF a poorer electron donor. This is again confirmed by the NBO analyses of HCF and H_2C. There is a higher percent C character in the occupied σ(C-H) orbitals of H_2C than in the σ(C-F) and σ(C-H) orbitals of HCF. Also, there is a higher electron density in the carbon lone pair orbital n(C) of H_2C than that of HCF. Thus H_2C is a better Lewis base than HCF. Overall, the Lewis acid-base interaction for the fragments of **1** is stronger than that for the fragments of **2**, which correlates with the isomers' positions in the order of stability.

A second qualitative analysis of the relative stabilities of **1** and **2** is obtained by comparing the bonds broken and formed as **1** is converted to **2**. In this conversion, B-F and C-H bonds are broken and B-H and C-F bonds are formed. The $\Delta_{rx}H$ values found in

the thermodynamic scheme below are calculated with reactant and product enthalpies of formation for the NIST chemistry webbook.[58]

BF → BH	$\Delta_{rx}H$ = 559 kJ/mol
CH → CF	$\Delta_{rx}H$ = - 339 kJ/mol
BF + CH → BH + CF	$\Delta_{rx}H$ = 220 kJ/mol

From these data we see that the endothermicity of the reaction **1** → **2** arises largely from the greater strength of the B-F bond compared to that of the B-H bond.

Interaction Energies. An aspect of borane(1) chemistry that has been explored previously in the group is the possibility of formation of HB···X complexes. Recognizing $HBCN^-$, HBCO and $HBCF^+$ as borane(1) complexes, Pappová et al.[20] evaluated the binding energies of these systems in terms of the BH affinities of the relevant diatomic species. Accepting this description, HCF···BH **7**, with a BH affinity of 7 kJ/mol, is a very weakly bound BH complex for which X equals F-bonding FCH. In contrast, when X equals C-bonding FCH in **2**, the BH affinity of 477 kJ/mol (Table 4) is indicative of tight B-C bonding and a new and different chemical compound. $HBCN^-$ and $HBCF^+$ were also viewed as new chemical compounds, and the BH affinity of **2** is significantly larger than the values obtained for $HBCN^-$ (248 kJ/mol) and $HBCF^+$ (293 kJ/mol) with a smaller basis set.[20] Moreover, the B-C bond strength in **2** is comparable to the bond strength of 462 kJ/mol calculated for the B-C bond in **1** (Table 4).

Consistent with the weak interaction between the fragments in **7**, there is very little donation of electron density from the HCF fragment to BH. The NBO analysis for this isomer gives a total hyperconjugation energy of merely 12.75 kJ/mol. The main contributors to the hyperconjugation interaction are two different n(F)→n*(B)

interactions; they account for 2/3 of the HCF interaction energy. The B-H fragment contributes 2.2 kJ/mol of hyperconjugation energy via a n(B)→σ*(C-H) interaction.

There are essentially two classes of hydrogen bonds, conventional or proper hydrogen bonds and unconventional or improper hydrogen bonds. Conventional hydrogen bond formation results in X-H bond lengthening in the hydrogen-bonded complex, X-H···Y, compared to the subunit X-H. In an improper hydrogen bond, the X-H bond actually shortens. Improper hydrogen bonding has been observed primarily for C-H bonds but has also been reported for Si-H,[58] P-H,[58] and even some N-H[58,59] bonds. Alabugin et al.[50] suggest that there are two competing influences that determine whether a hydrogen bond is proper or improper. X-H bond lengthening results from an n(Y)→σ*(H-X) hyperconjugative interaction and is balanced by X-H bond shortening caused by an increase in the s-character and polarization of the X-H bond. Improper hydrogen bonding is likely to occur only when the energy associated with the n→σ*(X-H) hyperconjugation ΔE(n→σ*) is smaller than the threshold value of 13-20 kJ/mol.[50] The hydrogen bond in HCH···FB **4** is very weak. It has a bond strength of 1.82 kJ/mol, which was evaluated by taking the sum of the total energies of the fragments and subtracting the total energy of the complex. This hydrogen bond is another example of an improper hydrogen bond. The C-H bond length in the complex is 0.0008 Å shorter than the corresponding length in the CH_2 molecule. ΔE(n(F) → σ*(C-H)) is 0.3 kJ/mol, well beneath the threshold value cited by Alabugin et al.[50] The percent s-character on the carbon in the σ(C-H) orbital increases from 21.65% for CH_2 to 21.79% for **4** and is apparently the predominant factor. These changes in bond length and % s-character are similar in magnitude to those found by Alabugin et al.[50]

Although uncoventional hydrogen bonds tend to be relatively weak, the bond in **4** is weaker than most. It is comparable in strength to the uncoventional hydrogen bonds in complexes of alcohols with Ne or CF_4 but considerably weaker than those in complexes of CF_3H with FH, ClH, H_2O, H_2S, and NH_3.[50] Surprisingly, the interaction in HCH···FB **4** is even weaker than that in the heterodimer HCF···BH **7**, which has a binding energy of 6.60 kJ/mol.

As pointed out by Weinhold and coworkers,[50] the ultimate example of a bond incapable of changing the percent s-character on the X atom is the H-H bond. According to their model, all H-H···Y complexes should have a longer H-H bond than H_2, even though $\Delta E(n \rightarrow \sigma^*)$ is below the threshold energy. This is precisely what they observe; the H-H bond shortens in all three of the complexes studied, namely H-H···OH_2, H-H···OMe_2 and H-H···Cl^-.[50] We have obtained similar results for H-H···C(F)B **8**. The main bond lengthening interaction (σ(C-B) $\rightarrow$ σ^*(H-H)) has a value of 1.50 kJ/mol, which is significantly below that of the 13-20 kJ/mol threshold. The H-H bond elongates by 0.0007 Å when the complex is formed. The interaction energy for **8**, 14.93 kJ/mol, is also comparable to that for H-H···Cl^-.[50]

Transition States. Table 6 lists the zero-point energy corrected total energies ZPE+E for the transition structures and the minima they connect. Due to the difficulty in calculating single point energies for the transition structures, we only have MP2 energies for them, so we have also listed the MP2 energies for the connected minima. Figure 6 is a potential energy diagram for [B, C, F, H_2]. Table 6 and Figure 6 also include the barriers for the given conversions, both in the forward and reverse directions. The lowest barrier is between **2** and **TS1-2**. At 53.8 kJ/mol, this barrier is still conceivably high

enough at the temperatures Andrews and his colleagues work with—typically around 6-7 K, annealing up to 25 and 35 K—that isomers other than **1** could be observed experimentally, given an appropriate pathway for their formation.

If **3** can be formed, there would be two main pathways for interconversion, **3** → **2** and **3** → **1**, with activation barriers of 82.7 kJ/mol and 106.1 kJ/mol respectively. At low temperatures, the rearrangement would follow the pathway through **TS2-3** because of the difference of about 23 kJ/mol in barrier heights. However, given the exothermicity of the reaction **3** → **2** (about -110 kJ/mol), it is conceivable that **2** would react further to form **1** as the final product. At higher temperatures, direct conversion of **3** → **1** would become competitive. The heights of the barriers indicate, however, that if **3** can be formed it may be stable at room temperature.

Frequencies. Table 5 lists the calculated MP2 and QCISD vibrational frequencies for each of the [B, C, F, H_2] structures. Structure **9** only has the MP2 frequencies because we have only been able to locate an MP2 minimum for that connectivity. The table also includes the observed frequencies from the laser ablation experiment with B + CH_3F by Andrews and Lanzisera.[3] In their more limited DFT study of the [B, C, F, H_2] PES, Lanzisera and Andrews considered only **1**, **2** and BH_2CF as possible isomers. From this more limited study, they found evidence for only H_2C-B-F, **1**, in their reaction of B with CH_3F.[3] Lanzisera and Andrews give the range of 1900-1700 cm^{-1} for C=B bond stretching and correlate the observed frequency of 1762.2 cm^{-1} with their calculated value of 1770.5 cm^{-1} from the DFT optimization of CH_2BF. Another experimental C=B frequency, 1822.3 cm^{-1} is identified with the 1854.1 cm^{-1} calculated frequency of CHBF, the other structure located in the experiment. Our calculated

frequency of 1753.4 cm^{-1} comes to within .5% of the observed frequency for CH_2BF. All other structures have B-C stretching frequencies that fall within 1300-1600 cm^{-1} and from their normal modes, appear to involve a mixture of stretching of the BC bond and bending or stretching of some other C-X bond, where X is either H or F. Unfortunately, the weak intensities associated with these absorptions make them unsuitable to rule out these isomers as products, since the absorptions may not be observed experimentally. However, each isomer **2-8** has a unique, strong absorption in a region of the spectrum where no peak was found experimentally. So, our more extensive analysis of the PES of [B, C, F, H_2] reinforces the conclusion by Lanzisera and Andrews that the reaction of B + CH_3F forms no isomer other than **1**.

The reason structures other than CH_2BF were considered as possible products of the B + CH_3F reaction is that Andrews and coworkers have studied several reactions for which products with a wide range of stabilities have been identified. If there is a viable boron insertion process and the barrier for conversion to the more stable form is high enough, then it is possible for much higher energy (less stable) structures to exist.[1] For instance, BNO is thought to be produced in the initial step of the reaction of B with NO. Further isomerization yields NBO, which is around 70-80 kcal/mol lower in energy than BNO.[60] Also, in their reaction with B and NO, Zhou et al.[1] found that BBNO and BBBNO nitrosyls are formed in addition reactions with B_2 and B_3. After annealing, these rearrange to the linear BNBO and BNBBO molecules which are calculated to be 137.4 kcal/mol and 162.2 kcal/mol more stable than the linear BBNO and BBBNO isomers.

If **2** or **3** were formed from the reaction of B + CH_3F, their production would involve insertion of B into a C-H bond. Similarly to **1**, **5** can be formed via insertion of B into the C-F bond but requires subsequent H atom rearrangement. Formation of each of the remaining isomers would require even more extensive atom rearrangements. Thus, the most likely products are **1**, **2** and **3**. While Andrews and coworkers have reported that C-H insertions occur in reactions of boron with CH_4 and other alkanes,[5,7,8] they interpret their results for the B + CH_3F reaction as indicating that this type of insertion appears to be sufficiently less favorable than a C-F insertion that it does not occur for this reaction. The calculated energy barriers for the **3** → **1**, **3** → **2** and **2** → **1** conversions (Figure 6) suggest that, at the temperatures at which these experiments are performed, **2** and **3** would be isolable if produced in this reaction. Thus our results support Andrews' and coworkers' interpretation. However, this is not to say that the other isomers cannot exist, only that they are not formed through this reaction.

Proton Affinities. By using the same levels of calculation for the $[B, C, F, H_3]^+$ and [B, C, F, H_2] systems, we were able to combine the data to compute proton affinities for several of our minima. Although, in principle, the C, B and F atoms can be protonated for each of the neutral isomers, relatively few of these possible protonations lead to stable $[B, C, F, H_3]^+$ ions. Of the ten minima located in the prior study, five have analogous structures in the neutral [B, C, F, H_2] system. The protonation reactions are represented in Figure 7. From these reactions we were able to obtain information on the protonation sites for the various analogs. Proton affinities ranged from about 900 kJ/mol to around 1400 kJ/mol. H_2CBF, **1**, is protonated at two sites, carbon and fluorine, and protonation at carbon is 430 kJ/mol more favorable than at fluorine. F-CH-BH, **2**, also

protonates at two sites, boron and fluorine; in this case, protonation of the boron is 159 kJ/mol more favorable than that of fluorine. The other two minima are only protonated at one site, **3** protonates at fluorine, whereas **5** protonates at carbon. Carbon is the most favored protonation site, followed by boron and then ending with fluorine. This trend parallels the results from a similar study of the proton affinities of monohydride and monofluoride derivatives of B, Al, N, and P. [13] Rozas et al. also found that carbon is a more favorable protonation site than boron which is more favorable than fluorine.[13]

B. [B, N, O, H_2]

1. Structures

Minima. For [B, N, O, H_2], 38 cyclic, linear, bent or hydrogen-bonded arrangements of these five atoms were examined, for some of which different point groups were explored. We have so far disclosed fifteen minima on the singlet potential energy surface. The 15 isomers are illustrated in Figure 8 and are also ordered with respect to decreasing stability. Three of the minima have a N-B-O connectivity, five have a B-N-O connectivity and three have a B-O-N connectivity. Zhou et al.[1] also found each of these types of arrangements in their investigation of the reactions of B atoms and clusters with NO. For example, NBO, BBNO and OBON molecules were formed in those reactions.

For [B, N, O, H_2] the most stable isomer again has the connectivity expected from chemical intuition H_2NBO, **1'**. Rearrangement of the boron and oxygen atoms yields isomer **7'** H_2NOB, whereas rearrangement of a H atom yields **2'** HOBNH. Although no equivalent structure with a BH_2 connectivity was located for the CF system, both H_2BNO **6'** and H_2BON **11'** were located. Likewise, H_2ONB **12'** and H_2OBN **15'** are minima.

We found one cyclic system **3'** *c*-HB-O-NH, for which AIM analysis identifies a bond critical point between each pair of atoms and also identifies a ring critical point. There are two hydrogen bonded systems, O-B-H···NH **10'** and BOH···NH **13'**. The first, **10'**, is a linear molecule, whereas **13'** has a bent geometry. The hydrogen bond in **13'** is a conventional O-H···N bond. In **10'**, the interaction is less conventional since the proton-donating atom is boron rather than oxygen. The heterodimer, HNO ─ B-H **14'**, a weak complex between borane(1) and HNO, is analogous to **7** and HO-N(H)-B **8'** is structurally very similar to **6** FH-B(H)-C. Stronger complexes involving borane(1) are found in HONBH **4'**, *bent*-HONBH **5'**, and HNOBH **9'**.

Table 7 lists the geometrical parameters of the isomers, including bond lengths, bond angles and bond dihedrals. O-H and B-H bond lengths are fairly consistent among the isomers. With the exception of the hydrogen donor O-H bond in **13'**, the O-H bond lengths cluster around 0.97 Å for both MP2 and QCISD geometries. The O-H bond in **13'** lengthens to 0.996 Å (MP2) or 0.982 Å (QCISD), which is characteristic of conventional hydrogen bonds. B-H bond lengths also follow a similar trend, clustering around 1.18 Å, with the exception of the heterodimer **14'** bond lengths which are slightly longer at around 1.24 Å and more typical of a B-H fragment (see also the B-H bond in **7**). The N-H bond distances are more variable; they range from about 1.0 Å in **2'** to about 1.06 Å in **14'**. The N-B, B-O and N-O bonds also show a wide variety of bond lengths consonant with the possibility of multiple bonding in some of these systems.

As in the [B, C, F, H_2] system, the magnitudes of the bond lengths and bond angles are generally consistent between the MP2 and QCISD levels of calculation. The direction in which bond distances vary between the levels is dependent on bond type; for

instance, all of the B-H bond lengths increase at the QCISD level, whereas all of the O-H bond lengths decrease at the higher level. There is also no overall consistency for bond angles. The majority of B-H, N-H, B-N, O-B, and O-H bonds differ by no more than 0.01 Å between the two levels. For these types of bonds, the exceptions to the 0.01 Å differences are few, especially when the heavy atoms are in N-B-O order. The main exceptions are the B-N bond in **15'** and the O-B bond in **5'**, with disagreements of 0.018 Å and 0.062 Å respectively. The largest discrepancy is seen in the H…N hydrogen bond which varies by 0.115 Å. In contrast, O-N bonds showed considerably worse agreement between levels of theory; differences range from 0.002 Å to 0.162 Å. For the most part, the bond angles do not vary by more than four degrees and most variations do not exceed one degree. There are, however, differences as large as 7° in **5'** and 14° in the heterodimer **14'**. Nevertheless, overall we do not see as dramatic a difference in bond lengths or angles between the two calculational levels as are seen for the [B, C, F, H_2] system.

Multiple Bond Character. Evaluation of the delocalized molecular orbitals for the [B, N, O, H_2] system suggests the likelihood of multiple bonding in the N-O, B-O, and/or B-N bonds of several of the isomers. Again using the convention of placing the heavy atoms in the XY plane, multiple bonding is indicated when there is an attractive interaction between the p_z atomic orbitals of the heavy atoms in one of the occupied orbitals and no analogous repulsive interaction in one of the remaining, higher energy occupied orbitals. Figure 9 shows the molecular orbital pictures for the overlaps mentioned below. For the N-O bond, MO 8 (Fig. 9A) of BH_2NO **6',** for example, has p_z atomic orbital (AO) coefficients of 0.356, 0.192 for N and 0.405, 0.280 for O. The p_z AO

coefficients for N and O in MO 8 (Fig. 9B) of HO-N-BH **4'** are similar at 0.272, 0.140 and 0.549, 0.373 for N and O respectively. However, MO 11 of **4'** shows an antibonding interaction between N (0.439, 0.315) and O (-0.353, -0.292) not observed for **6'**. Similar analysis gives evidence for NO multiple bond character in **11'** (Fig. 9C) and **14'** (Fig. 9D).

Likewise, B-O multiple bonds are indicated for isomers NH_2BO **1'**, NH_2OB **7',** HNOBH **9'**, and OBH···NH **10'**. The p_z coefficients for B (0.259 and 0.0373) and for O (0.545 and 0.360) in MO 10 (Fig. 9E) of **1'** are typical of those observed for each of these four molecules. The electron density in these MOs is skewed more toward the oxygen than it tends to be in the corresponding MOs for N and O. With the smaller difference in electronegativity for B and N than for B and O, there is generally less distortion of the electron density toward N in the MOs comprised of primarily attractive Np_z and Bp_z contributions. This MO for HONBH **4'**, MO 8, has Np_z coefficients of 0.439 and 0.315 and Bp_z coefficients 0.312 and 0.140. Three other configurations have similar attractive B-N interactions, namely HOBNH **2'**, OH_2NB **12'** and OH_2BN **15'**. Zhou et al. also found evidence for B-N, B-O and N-O multiple bonding in the products of the B_n + NO reactions: NBO, BNBO and $BNBO^-$, OBNNO, BBNO, BBBNO, BNBBO, $NNBO_2$ and OBON.[1]

The AIM analysis of the [B, N, O, H_2] systems provides additional support for multiple bonding. Table 8 gives the B-O, B-N, and N-O bond orders and bond densities calculated with this technique. Potential bonds for which the AIM analysis did not locate a bond critical point are not included in the table, e.g. the B-O bond in **5'**. Bond order entries missing from the table indicate that the AIM analysis did not work completely.

The data show a significant increase in both bond order and bond density for those B-O, B-N and N-O bonds suggested to have multiple bonds.

2. Energetics

Minima. Table 9 lists the calculated energies, zero-point corrected energies, enthalpies and free energies for the [B, N, O, H_2] minima. Table 10 gives connectivities and relative energies, based on energies from Table 9, for the 15 isomers. The difference in total energies (QCISD(T)//QCISD) between the most stable structure, H_2NBO **1**', and the second most stable, HO-B-NH **2'** is about 85.1 kJ/mol. This is about 1/3 of the difference seen for the first two structures in the [B, C, F, H_2] system. The energy deviation between the most and least stable, H_2O-B-N, **15**', is 847 kJ/mol, which is about 100 kJ/mol larger than the CF system. For the three possible arrangements of N, B, and O: NBO, BNO and BON, Zhou et al.[1] found that structures with a N-B-O connectivity are most stable, followed by B-N-O and B-O-N in order of stability. We also see this trend. The two most stable structures have a NBO arrangement. The lowest energy BNO structure **4'** is about 330 kJ/mol less stable than **2'**; the lowest energy NOB structure **7'** is about 410 kJ/mol less stable than **2'** and about 80 kJ/mol less stable than **4'**.

*Isomer **1'** versus **2'**.* On the basis of the analysis of the delocalized MOs, the AIM analysis and the NBO analysis, reasonable Lewis structures for **1**' and **2'** are:

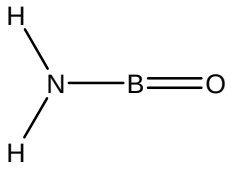

1'

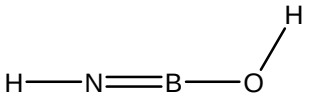

2'

Given these structures, the relative energy of **2'** with respect to **1'** can be qualitatively understood by evaluating the net change in energy associated with breaking

a N-H bond and B-O bond and forming a O-H and B-N bond. The thermodynamic scheme given below will give us only an estimate for the overall energy change since diatomic BO and BN are multiply bonded. Nevertheless, it is instructive. Again the $\Delta_{rx}H$ values were obtained from the experimental enthalpies of formation for the reactants and products. The enthalpy of formation of BO is from Gurvich et al.[61] The remaining enthalpies of formation are from the NIST chemistry webbook.[58]

NH → OH	$\Delta_{rx}H$ = - 335 kJ/mol
BO → BN	$\Delta_{rx}H$ = 470 kJ/mol
NH + BO → OH + BN	$\Delta_{rx}H$ = 135 kJ/mol

The thermochemical data suggest that the rearrangement of **1'** to **2'** is endothermic because of the large cost in energy required to convert the BO bond to a BN bond.

Interaction Energies. For the [B, N, O, H_2] system, *c*-HBONH **3'**, HONBH **4'**, *bent*-HONBH **5'**, HONBH **9'** and HNO—BH **14'** can all be considered borane(1) complexes in which BH functions as a Lewis acid. In **3'**, BH binds to both the N and O atoms, and in **9'** it binds to the O atom. The Lewis base is N-bonded NOH in **4'** and **5'**. With a BH affinity of 21 kJ/mol (Table 11), the interaction between HNO and BH in **14'** is considerably stronger than that for the heterodimer HCF···BH **7**. The main hyperconjugations that contribute to the BH affinity of **14'** HNO···BH are a n(B) → σ*(H-N) interaction and a σ(B-H)→ σ*(H-N) interaction from the B-H subunit and two n(O) → n*(B) interactions, a σ(N-O)→n*(B) interaction, and a n(O)→σ*(B-H) interaction from the HNO subunit. The total hyperconjugation energy is 265.5 kJ/mol. In contrast, the interaction between BH and N-bonded NOH is 523.5 kJ/mol for **4'** and 503.8 kJ/mol for **5'**, comparable to the 497.3 kJ/mol calculated for FCHBH **2**. Consistent with the poorer electron donating ability of oxygen with respect to nitrogen, the BH

affinity of O-bonded HNO in **9'** is much smaller at 294.5 kJ/mol, similar in magnitude to those for CF^+ and CN^-.[20] The strongest interaction is observed for BH and N- and O-bonded HNO at 553.3 kJ/mol, but the relatively small increase in affinity compared to that of HONBH **4'** is indicative of the ring strain in *c*-HBONH **3'**.

The hydrogen bond in OBH···NH **10'** is considerably stronger than that of the CF hydrogen bonded structure **4.** The strength of the hydrogen bond in OBH···NH **10'** is 6.67 kJ/mol. **10'** has a n(N)→σ*(B-H) hyperconjugation energy of 11.4 kJ/mol; this is below the threshold range given by Alabugin et al.[50] This hyperconjugation energy, along with a .0016 Å decrease in B-H bond length compared to the corresponding OBH fragment and an increase from 27.93 % to 28.17 % in overall s-character of the boron in the B-H bond, suggests that, like **4,** the hydrogen bond in **10'** is an unconventional one. For **13'** the s-character of the oxygen in the O-H bond increases from 23.13 % in the fragment to 27.78 % in the complex. Nevertheless, the O-H bond lengthens by 0.0134 Å with respect to the fragment, due to the overwhelming n(N)→σ*(O-H) hyperconjugation energy, totaling 135.4 kJ/mol—well beyond the threshold range.[50] Thus the hydrogen bond in **13'** is conventional.

Frequencies. Table 12 collects the calculated MP2 and QCISD normal mode vibrational frequencies for each [B, N, O, H_2] minimum. To our knowledge, there has been no published experimental study of [B, N, O, H_2]. So there is certainly an interest in collaboration with an experimentalist to perform reactions of laser-ablated boron atoms with a suitable starting material. Perhaps NH_2OH + B would be a viable reaction. Following Andrews' and coworkers' proposed mechanism,[3] the boron would have three possible insertion sites: the N-H, N-O, and O-H bonds. The possible products would be

1'-4' and **7'-9'** (See Figure 10). That is, seven of the 15 minima we have already disclosed may be formed via the proposed bond insertion/hydrogen abstraction mechanism. This possibility coupled with the already decreased separation between the first and second most stable minima suggest that more than one isomer may be isolable in a matrix isolation experiment. Although there are no experimental data for the [B, N, O, H_2] system, Zhou et al. have performed reactions of B with NO and have seen nine novel structures containing N-B, N-O and B-O bonds.[1] Table 13 lists relevant frequencies from Zhou et al.[1] For the sake of brevity, only a few calculated frequencies will be compared with typical absorptions observed for B-O and N-O stretches. The B-O stretching frequencies reported by Zhou et al.[1] are regularly around 2000 cm^{-1}. The B-O stretching frequency of 1987 cm^{-1} that we see for **1'** is in good agreement with this value. The band observed at 1149 cm-1 for OBON (Table 13) is consistent with an N-O stretch in an isonitrosyl structural arrangement.[1] We find a similar vibrational frequency, 1142 cm^{-1}, for NH_2OB **7'**. The band position for the terminal N-O stretching of a nitrosyl group is higher at about 1900 cm^{-1} (Table 13).[1] The corresponding calculated frequency is 1885 cm^{-1} for BH_2NO **6'**. The good agreement between the experimentally observed and calculated frequencies, for both [B, C, F, H_2] and [B, N, O, H_2], suggests that the calculated frequencies could be utilized to help with the assignment of observed bands. The unique set of strong absorptions for each of the [B, N, O, H_2] isomers (Table 12) should allow for its identification if formed as a reaction product.

SYSTEM COMPARISON

Geometries. There are a few differences between the two systems. HN-O-BH **3**' is a cyclic molecule whereas no cyclic arrangements were stable for the [B, C, F, H_2]

system. Also, as mentioned above, we have two minima of the form H_2B-X-Y: H_2B-N-O **6**' whose analogous structure, H_2B-C-F is a transition state, **TS2-2**, and H_2B-O-N (**11**') whose analogous structure H_2B-F-C is unstable. Similarly NH_2OB **7'**, the analog of CH_2FB, is stable whereas the CF structure is not. A possible reason for the latter results may also be one of the reasons why the [B, N, O, H_2] system has produced more minima than the [B, C, F, H_2] system. Carbon has a tendency to form four bonds; one can draw a Lewis structure for CH_2FB where carbon has four bonds and formal charges are minimized, but to do so fluorine, which is already bridged, has to have a double bond. Fluorine's small size causes its electrons to be more tightly held (high electronegativity) so removing electron density from the fluorine is not favorable. Therefore, the plausibility of three bonds on fluorine is low. On the other end, boron is electron poor and cannot compensate for the electron density lost by fluorine in forming a multiple bond with carbon and a single bond with the boron. In contrast, with NO, neither nitrogen nor oxygen tends to form four bonds and both form multiple bonds more readily than fluorine (smaller electronegativities). Consequently, NH_2OB **7'** is a minimum and CH_2FB is not.

Energetics. Tables 3 and 9 list the relative QCISD(T)//QCISD energies for the CF and NO systems, respectively. As you can see, the differences in energy between the first and second structures are vastly different. The difference in energy between the first and second minima for the CF system is nearly three times that of the NO. One wonders why this is; why is the second structure of the CF system so much less stable in relation to the second structure for the NO system? Recall that to form **2** from **1**, one must break BF and CH bonds to form BH and CF bonds. This results in an estimated overall

$\Delta_{rx}H$ = 220 kJ/mol. For the conversion of **2'** from **1',** one breaks NH and BO bonds to form OH and BN bonds. The overall enthalpy for this process estimated as $\Delta_{rx}H$ = 135 kJ/mol. The process for the CF system requires about 85 kJ/mol more than that for the NO system. The transitions from CH → CF and NH → OH have similar energy requirements, so the real controlling factor is that more energy is needed to break BF than what is recovered by forming BH compared to what is needed to break BO and recovered by forming BN.

FUTURE WORK

For the [B, C, F, H_2] system, we have essentially finished our investigation of the minima on the singlet potential energy surface. We will search for more transition structures, but it might prove more profitable to begin investigating the triplet potential energy surface. Starting with the existing minima, it would be interesting to determine if any of them exist in a lower energy state on the triplet PES. We would also investigate those structures, such as BH_2CF, that were not minima as singlets.

There is still much to do for the [B, N, O, H_2] system. We have not completely exhausted the available connectivities for consideration, nor have we begun to examine the transitions between stable minima.

As another extension of this work, one might also consider the valence isoelectronic system [B, N, S, H_2]. What sorts of structures would we see? Will they be similar to those seen for the NO or CF system? Will there be an even greater number of minima? Might there be a further depression of the separation between the first and second most stable minima? Would one see more cyclic minima? Will there be an increase in multiple bond character?

Table 1: [B, C, F, H_2] Geometries; Bond Lengths (Å) and Angles (degrees).[a,b]

Structure	Bond Lengths		Bond Angles		Dihedral Angles	
[CH_2BF], 1	R (C, H)	1.092	A (B, C, H)	121.1		
		1.093		121.3		
C_{2v}	R (C, B)	1.399	A (H, C, H)	117.3		
		1.401		117.4		
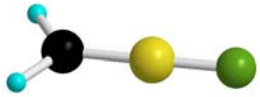	R (B, F)	1.313				
		1.313				
[CHFBH], 2	R (C, F)	1.382	A (H, C, F)	113.2		
		1.383		112.8		
C_s	R (C, B)	1.418	A (F, C, B)	124.0		
		1.420		123.2		
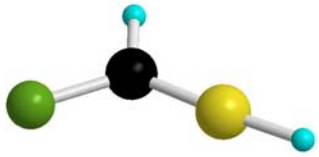	R (B, H)	1.180	A (H, C, B)	122.8		
		1.183		123.9		
	R (C, H)	1.095	A (H, B, C)	176.0		
		1.096		176.5		
[CH_2FB], 3	R (C, H)	1.106	A (H, C, H)	108.7	D(H, C, B, F)	118.8
tetrahedral		1.108		108.6		118.8
	R (C, B)	1.603	A (F, C, H)	108.5	D(H, C, F, B)	121.0
C_s		1.691		108.3		121.2
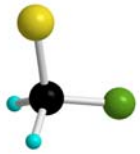	R (C, F)	1.422	A (B, C, H)	112.0	D(H, C, F, H)	117.9
		1.421		112.2		117.6
			A (F, C, B)	107.0	D(H, C, B, H)	122.3
				107.2		122.5
[HCH···FB], 4	R (C, H)	1.119	A (H, C, H)	101.7		
		1.125		101.3		
C_s	R (H···F)	2.863	A (C, H···F)	114.5		
		2.793		126.1		
	R (F, B)	1.303	A (H···F, B)	172.7		
		1.308		174.9		
[HCBFH], 5	R (C, H)	1.083	A (H, C, B)	151.7		
		1.085		149.8		
C_s	R (C, B)	1.356	A (C, B, F)	134.4		
		1.367		127.1		
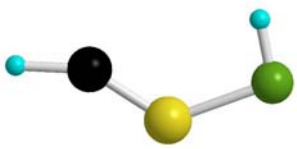	R (F, B)	1.593	A (B, F, H)	97.0		
		1.629		98.8		
	R (F, H)	0.949				
		0.941				

Table 1: [B, C, F, H_2] Geometries; Bond Lengths and Angles cont.

Structure	Bond Lengths		Bond Angles		Dihedral Angles	
[CBHFH], 6	R (C, B)	1.475	A (C, B, H)	167.0	D (H, B, F, H)	136.2
		1.478		169.0		133.3
C_1	R (B, H)	1.185	A (H, B, F)	105.1	D (C, B, F, H)	-44.0
		1.188		103.1		-46.8
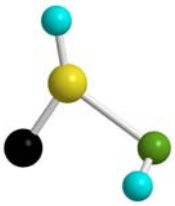	R (F, B)	1.912	A (B, F, H)	99.5		
		1.996		101.7		
	R (F, H)	0.941				
		0.934				
[HCF—BH], 7	R (C, H)	1.125	A (H, C, F)	101.2		
		1.133		101.3		
C_s	R (C, F)	1.342	A (C, F, B)	112.8		
		1.345		113.4		
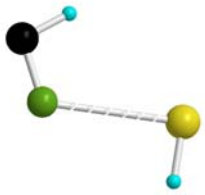	R (B, H)	1.241	A (F, B, H)	86.8		
		1.249		86.3		
	R (F—B)	2.836				
		2.963				
[HH···C(F)B], 8	R (H, H)	0.756	A (H···C, F)	82.3	D (H, H, C, F)	40.1
		0.762		79.4		0.0
C_1	R (H···C)	2.885	A (H, H···C)	165.3	D (H, H, C, B)	160.1
		2.990		164.2		180.0
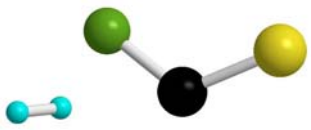	R (F, C)	1.334	A (F, C, B)	120.9		
		1.337		111.9		
	R (C, B)	1.455				
		1.682				
[HH···FCB], 9	R (H, H)	0.755	A (H···F, C)	148.9	D (H, H···F, C)	-178.7
C_s	R (H···F)	2.737	A (H, H···C)	173.6	D (H···F, C, B)	179.9
	R (F, C)	1.336	A (F, C, B)	120.8		
	R (C, B)	1.454				

[a] MP2 parameters in black, QCISD parameters in red. [b] Atom color scheme: C: black, H: turquoise, B: yellow, F: green.

Table 2: [B, C, F, H_2] QCISD(T)/aug-cc-pVTZ//QCISD/aug-cc-pVDZ Energies.[a]

STRUCTURE	QCISD(T)/QCISD	E0+ZPE	H 298	G 298
CH_2BF, 1	-163.7565673	-163.72806	-163.72324	-163.75154
CHFBH, 2	-163.6615113	-163.63403	-163.62935	-163.65853
CH_2FB, 3	-163.6241466	-163.59501	-163.59047	-163.61966
HCH···FB, 4	-163.5745383	-163.55450	-163.54655	-163.58665
HCBFH, 5	-163.5670086	-163.54052	-163.53510	-163.56555
CBHFH, 6	-163.5268837	-163.50305	-163.49711	-163.52913
HCF···BH, 7	-163.474618	-163.45574	-163.44837	-163.48538
HH···C(F)B, 8	-163.4570659	-163.44099	-163.43304	-163.47122
BH	-25.2314036	-25.2260996	-25.2227956	-25.2423286
BF	-124.509428	-124.506591	-124.503273	-124.52611
CH_2	-39.0644163	-39.0478343	-39.0440503	-39.0655563
HCF	-138.2407024	-138.2285154	-138.2247094	-138.2501094
FCB	-162.2789664	-162.2739374	-162.2705184	-162.2954414
H_2	-1.172414	-1.162514	-1.159209	-1.174049

[a] Energies in hartrees.

Table 3: [B, C, F, H_2] Relative Energies, Enthalpies and Free Energies.[a]

STRUCTURE	E0+ZPE	H 298	G 298
CH_2BF, 1	0.00000	0.00000	0.00000
CHFBH, 2	246.8746293	246.5123158	244.1861582
CH_2FB, 3	349.3140399	348.6025402	346.2317499
HCH···FB, 4	455.6722121	463.8977783	432.9094739
HCBFH, 5	492.3674789	493.9585077	488.3163941
CBHFH, 6	590.7589553	593.6994705	583.919632
HCF···BH, 7	714.9739312	721.6819815	698.7905958
HH···C(F)B, 8	753.6813505	761.9069167	735.9594955

[a] Relative QCISD(T)/aug-cc-pVTZ//QCISD/aug-cc-pVDZ energies in kJ/mol.

Table 4: [B, C, F, H_2] Fragmentation Energies.

Fragmentations	ΔE (kJ/mol)
1 → BF + CH_2	479.7319276
2 → BH + HCF	497.2760389
4 → BF + CH_2	1.82206924
7 → BH + HCF	6.59515552
8 → FCB + H_2	14.92705283

Table 5: [B, C, F, H_2] MP2 and QCISD Calculated Frequencies (cm^{-1}) and Intensities (km/mol).

Structure	MP2 Frequencies[a]	QCISD Frequencies[a]	Observed Frequencies[b]
[CH_2BF], 1, C_{2v}	b_2 307.0 (5.3), b_1 387.1 (17.6), b_1 592.6 (63.2), b_2 765.1 (43.6), a_1 886.6 (29.5), a_1 1324.7 (2.1) a_1 1753.4 (396.1), a_1 3201.7 (18.2), b_2 3301.0 (3.75)	b_2 315.8 (6.7), b_1 371.3 (12.2), b_1 622.1 (61.6), b_2 782.2 (40.4), a_1 883.1 (33.2), a_1 1341.3 (1.3), a_1 1751.0 (381.0), a_1 3177.0 (10.6), b_2 3269.5 (1.0)	b_1 589.5, b_2 755.0, a_1 917.4, a_1 1762.2, a_1 3050.2;[c] 590.2, 767.5, 919.5, 1822.0, 1822.3, 1884.7, 3261.7[d]
[CHFBH], 2, C_s	a' 285.0 (1.7), a" 536.9 (1.8), a" 684.8 37.8), a' 803.7 (47.2) a' 1009.3 (64.1), a' 1205.5 (23.7), a' 1530.9 (18.9), a' 2868.3 (4.3), a' 3215.7 (10.7)	a' 293.0 (2.1), a" 505.1 (2.8), a" 686.3 (34.7), a' 799.1 (44.5), a' 1011.0 (66.1), a' 1211.8 (21.8), a' 1528.0 (18.9), a' 2829.2 (4.6), a' 3199.8 (8.2)	
[CH_2FB], 3, C_s	a' 239.1 (28.2), a'' 585.0 (28.9), a' 849.8 (87.3), a' 1030.9 (52.7), a'' 1197.5 (0.1), a' 1315.6 (29.0), a' 1420.8 (19.4), a' 3054.1 (21.4), a'' 3124.3 (3.9)	a' 256.5 (23.6), a'' 603.9 (24.3), a' 840.3 (85.2), a' 1029.3 (60.0), a'' 1201.1 (0.0012), a' 1318.0 (21.4), a' 1426 (15.2), a' 3026.1 (22.2), a'' 3087.1 (8.6)	
[CHH···FB], 4, C_s	a' 17.7 (3.5), a' 52.5 (8.8), a" 57.9 (70.6), a" 69.0 (5.9), a' 80.0 (58.1), a' 1264.2 (204.6), a' 1409.4 (1.3), a' 2976.5 (72.7), a' 3059.6 (75.8)	a' 18.3 (11.0), a' 45.3 (8.1), a" 48.1 (34.2), a" 71.1 (15.8), a' 79.9 (41.9), a' 1242.9 (218.4), a' 1401.6 ((0.65), a' 2906.7 (81.7), a' 2981.2 (93.0)	
[HCBFH], 5, C_s	a' 218.3 (106.9), a" 245.9 (83.9), a' 539.8 (23.0), a' 614.9 (77.1), a" 619.9 (5.8), a' 757.0 (218.3), a' 1646.9 (19.1), a' 3378.2 (8.7), a' 3710.1 (238.1)	a' 240.5 (101.4), a" 246.3 (86.5), a' 504.7 (51.3), a" 558.3 (33.1), a' 631.0 (48.9), a' 729.2 (253.2), a' 1544.4 (32.7), a' 3348.3 (3.2), a' 3822.5 (185.1)	
[CBHFH], 6, C_1	a 166.8 (136.3), a 240.5 (80.9), a 281.7 (44.0), a 526.7 (230.9), a 630.0 (35.1), a 785.7 (122.3), a 1303.7 (4.4), a 2829.0 (15.8), a 3800.4 (137.2)	a 158.8 (123.4), a 211.7 (76.3), a 242.4 (45.1), a 503.4 (203.3), a 590.5 (31.8), a 749.8 (115.2), a 1289.8 (2.8), a 2791.8 (15.9), a 3923.8 (142.8)	
[HCF−BH], 7, C_s	a' 68.7 (17.5), a" 88.6 (26.1), a' 106.4 (8.7), a" 125.0 (128.2), a' 303.4 (47.5), a' 1121.8 (185.0),	a' 59.8 (14.1), a" 71.1 (39.4), a' 89.3 (6.5), a" 104.5 (83.7), a' 256.7 (35.3), a' 1108.2 (172.9),	

	a' 1427.8 (24.1), a' 2424.3 (362.1), a' 2920.4 (84.5)	a' 1412.3 (21.2), a' 2346.8 (370.4), a' 2838.9 (111.0)	
[HH···C(F)B], 8, C_1	a 24.4 (1.8), a 51.4 (0.24), a 130.8 (0.61), a 227.2 (2.0), a 242.6 (4.1), a 405.3 (97.8), a 1005.2 (46.3), a 1208.1 (944.8), a 4438.6 (2.5)	a 37.1 (0.50), a 39.8 (0.35), a 110.9 (0.52), a 186.3 (1.2), a 201.0 (58.4), a 256.5 (0.24), a 724.2 (137.7), a 1170.7 (130.0), a 4328.0 (7.4)	
[HH···FCB], 9, C_s	a 15.9 (1.2), a 20.7 (1.3), a 94.8 (0.35), a 202.6 (0.051), a 207.8 (.043), a 403.7 (99.0), a 1002.8 (56.4), a 1207.9 (992.6), a 4456.8 (3.3)		

[a] IR intensities in parentheses. [b] Reference 3. [c] Frequencies assigned to CH_2BF. [d] Other obs. frequencies.

Table 6: [B, C, F, H_2] Total Energies and Energy Barriers for the Forward and Reverse Interconversions.

Minima and Transition Structures	**E+ZPE[a]**	**E_a (kJ/mol)[b]**	**E_a' (kJ/mol)**
CH_2BF, 1	-163.5473202		
CHFBH, 2	-163.4559594		
TS1-2	-163.4354724	293.7	53.8
TS2-2	-163.4148025	108.1	108.1
CH_2FB, 3	-163.4137766		
TS2-3	-163.3822851	193.4	82.7
TS1-3	-163.3733716	456.7	106.1
HCBFH, 5	-163.3624157		
HCH···FB, 4	-163.3615989		
TS3-4	-163.3361591	203.8	66.8
TS2-5	-163.3052188	395.8	150.2

[a] MP2/aug-cc-pVDZ calculations. [b] E_a: Barrier in forward direction, E_a': Barrier in reverse direction.

Table 7: [B, N, O, H_2] Geometries; Bond Lengths (Å), Bond Angles (degrees) and Dihedral Angles.[a,b]

Structure	Bond Lengths		Bond Angles		Dihedral Angles	
[NH_2BO], 1'	R (N, H)	1.002	A (H, N, B)	120.2		
		1.012		123.2		
C_s	R (B, O)	1.233	A (N, B, O)	178.2		
		1.227		178.3		
	R (N, B)	1.400	A (H, N, H)	113.9		
		1.401		113.9		
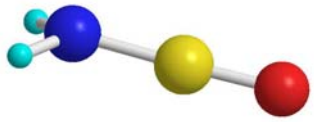						
[HOBNH], 2'	R (O, H)	0.966	A (O, B, N)	177.3		
		0.964		177.8		
C_s	R (N, B)	1.257	A (B, N, H)	179.9		
		1.253		179.1		
	R (N, H)	0.999	A (H, O, B)	113.6		
		0.998		113.7		
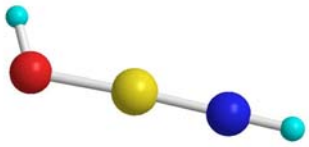	R (B, O)	1.358				
		1.357				
[*c*-HBONH], 3'	R (N, O)	1.650	A (N, O, B)	56.9	D (H, B, O, N)	177.6
		1.638		57.5		178.0
C_1	R (B, O)	1.352	A (O, B, N)	71.9	D (H, B, N, O)	-177.2
		1.345		71.4		-177.7
	R (B, H)	1.186	A (O, B, H)	140.5	D (H, B, N, H)	94.2
		1.189		141.1		93.3
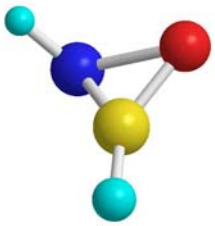	R (N, B)	1.455	A (H, N, B)	110.5		
		1.458		110.4		
	R (N, H)	1.030	A (B, N, O)	51.1		
		1.030		51.1		
[HONBH], 4'	R (O, H)	0.971	A (O, N, B)	170.7		
		0.969		170.2		
C_s	R (N, O)	1.348	A (N, B, H)	177.3		
		1.352		176.8		
	R (N, B)	1.246	A (H, O, N)	104.8		
		1.252		104.8		
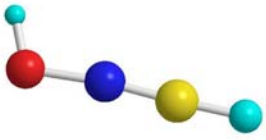	R (B, H)	1.176				
		1.179				
[*bent*- HONBH], 5'	R (O, H)	0.974	A (H, O, B)	109.3	D (H, O, B, H)	91.9
		0.970		110.2		92.9
C_1	R (O, N)	1.654	A (O, N, B)	62.8	D (H, O, B, N)	-88.6
		1.779		56.1		-87.8
	R (B, H)	1.182	A (H, B, N)	160.2	D (H, B, N, O)	178.7
		1.188		152.6		178.9
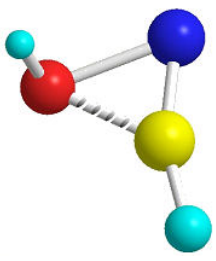	R (N, B)	1.342	A (H, B, O)	131.5		
		1.354		131.2		
	R (O, B)	1.583	A (H, O, N)	104.8		
		1.521		104.8		

Table 7: [B, N, O, H_2] Geometries; Bond Lengths and Angles cont.

Structure	Bond Lengths		Bond Angles		Dihedral Angles	
[BH_2NO], 6'	R (B, H)	1.198	A (H, B, H)	129.8		
		1.201		129.3		
C_{2v}	R (N, B)	1.353	A (H, B, N)	115.3		
		1.363		115.1		
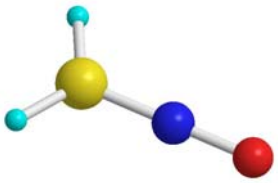	R (O, N)	1.193				
		1.186				
[NH_2OB], 7'	R (O, N)	1.491	A (H, N, O)	100.8		
		1.478		101.3		
C_s	R (N, H)	1.024	A (N, O, B)	106.1		
		1.025		110.5		
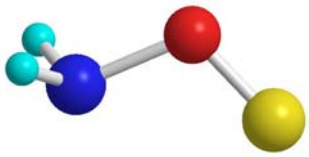	R (B, O)	1.347	A (H, N, H)	106.0		
		1.346		105.5		
[HN(B)OH], 8'	R (N, B)	1.411	A (B, N, H)	127.4	D (H, O, N, H)	98.0
		1.415		126.8		97.9
C_1	R (O, N)	1.422	A (B, N, O)	118.4	D (H, O, N, B)	-95.2
		1.420		118.8		-96.7
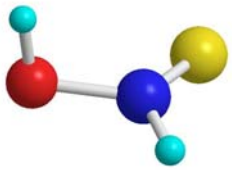	R (O, H)	0.971	A (H, N, O)	112.7		
		0.969		112.5		
	R (N, H)	1.019	A (N, O, H)	104.0		
		1.018		104.4		
[HNOBH], 9'	R (N, H)	1.033	A (H, N, O)	97.5		
		1.038		93.1		
C_s	R (O, N)	1.464	A (N, O, B)	164.2		
		1.626		159.8		
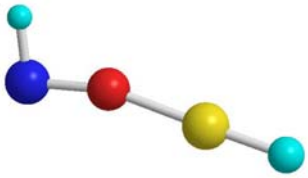	R (B, O)	1.223	A (O, B, H)	178.8		
		1.216		178.5		
	R (B, H)	1.173				
		1.178				
[OBH···NH], 10'	R (B, O)	1.224				
		1.217				
$C_{\infty v}$	R (B, H)	1.176				
		1.180				
	R (H···N)	2.607				
		2.624				
	R (N, H)	1.041				
		1.045				

Table 7: [B, N, O, H_2]Geometries; Bond Lengths and Angles cont.

Structure	Bond Lengths		Bond Angles		Dihedral Angles
[BH_2ON], 11'	R (B, H)	1.193	A (H, B, H)	130.7	
		1.197		130.5	
C_{2v}	R (B, O)	1.372	A (H, B, O)	114.6	
		1.379		114.7	
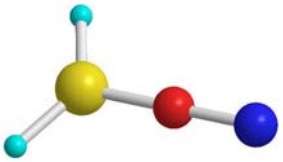	R (O, N)	1.227			
		1.229			
[OH_2NB], 12'	R (O, H)	0.975	A (N, O, H)	101.0	
		0.971		99.4	
C_s	R (O, N)	1.575	A (H, O, H)	106.8	
		1.666		106.5	
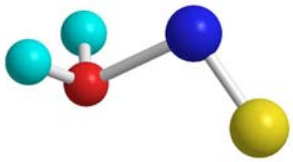	R (N, B)	1.407	A (O, N, B)	101.6	
		1.413		100.3	
[$BOH^{\cdots}NH$], 13'	R (B, O)	1.309	A (B, O, H)	124.3	
		1.316		122.9	
C_s	R (O, H)	0.996	A ($H^{\cdots}N$, H)	110.8	
		0.982		115.2	
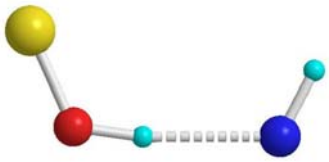	R ($H^{\cdots}N$)	1.812	A ($O^{\cdots}H$, N)	175.9	
		1.927		175.9	
	R (N, H)	1.042			
		1.045			
[HNO–BH], 14'	R (N, H)	1.062	A (H, N, O)	104.4	
		1.065		106.5	
C_s	R (O, N)	1.237	A (N,O–B)	107.4	
		1.221		107.7	
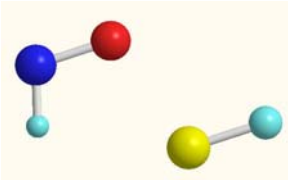	R (B, H)	1.234	A (O–B, H)	92.9	
		1.243		107.7	
	R (O–B)	2.019			
		2.216			
[OH_2BN], 15'	R (O, H)	0.975	A (H, O, B)	111.0	
		0.973		111.4	
C_s	R (B, O)	1.519	A (O, B, N)	176.9	
		1.520		176.4	
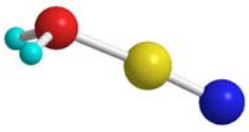	R (N, B)	1.288	A (H, O, H)	108.1	
		1.270		108.4	

[a] MP2 parameters in black, QCISD parameters in red. [b] Atom color scheme: N: blue, O: red, B: yellow, H: turquoise.

Table 8: [B, N, O, H_2] AIM Bond Orders and Bond Densities.

	Bond Order	**Bond Density**	**Minimum**	**type**
B-O	0.805	0.280	**1'**	B=O
	0.504	0.202	**2'**	B-O
	0.463	0.201	**3'**	B-O
	0.793	0.203	**7'**	B=O
	0.874	0.260	**9'**	B=O
	0.929	0.285	**10'**	B=O
	0.485	0.149	**11'**	B-O
	0.414	0.113	**15'**	B-O
	Bond Order	**Bond Density**	**Minimum**	**type**
N-O	1.208	0.177	**3'**	N-O
	1.269	0.352	**4'**	N-O
	1.131	0.166	**5'**	N-O
	2.070	0.519	**6'**	N=O
	1.118	0.241	**7'**	N-O
	1.038	0.216	**8'**	N-O
	1.771	0.430	**11'**	N=O
		0.181	**12'**	N-O
		0.469	**14'**	N=O
	Bond Order	**Bond Density**	**Minimum**	**type**
B-N	0.535	0.209	**1'**	B-N
	0.861	0.257	**2'**	B=N
	0.403	0.184	**3'**	B-N
	1.034	0.240	**4'**	B=N
	0.711	0.242	**5'**	B-N
	0.658	0.180	**6'**	B-N
	0.814	0.196	**8'**	B-N
		0.210	**12'**	B=N
	1.626	0.244	**15'**	B=N

Table 9: [B, N, O, H_2] QCISD(T)/aug-cc-pVTZ//QCISD/aug-cc-pVDZ Energies[a].

STRUCTURE	QCISD(T)/QCISD	E0+ZPE	H 298	G 298
NH_2BO, 1'	-155.8810931	-155.8490651	-155.8441911	-155.8731131
HOBNH, 2'	-155.8467502	-155.8166352	-155.8112132	-155.8409332
HBONH, 3'	-155.752438	-155.722878	-155.718668	-155.74686
HONBH, 4'	-155.7190087	-155.6898577	-155.6847417	-155.7138037
***bent*-HONBH, 5'**	-155.7104338	-155.6815098	-155.6770258	-155.7057428
BH_2NO, 6'	-155.7061933	-155.6798563	-155.6749793	-155.7033593
NH_2OB, 7'	-155.6918294	-155.6606084	-155.6556164	-155.6854134
HN(B)OH, 8'	-155.6615132	-155.6309282	-155.6259782	-155.6555472
HNOBH, 9'	-155.6538848	-155.6280228	-155.6223388	-155.6529208
OBH···NH, 10'	-155.6379304	-155.6147884	-155.6077524	-155.6420954
BH_2ON, 11'	-155.636053	-155.610592	-155.605545	-155.634337
OH_2NB, 12'	-155.5851918	-155.5557538	-155.5504268	-155.5809658
BOH···NH, 13'	-155.575319	-155.55213	-155.545489	-155.579933
HNO–BH, 14'	-155.5527583	-155.5290323	-155.5232323	-155.5550343
OH_2BN, 15'	-155.5579269	-155.5266069	-155.5214609	-155.5511029
BH	-25.2314036	-25.2260996	-25.2227956	-25.2423286
BOH	-100.4894619	-100.4732179	-100.4722739	-100.4972209
NH	-55.0755081	-55.0655251	-55.0645811	-55.0840851
HNO	-130.3103003	-130.2935203	-130.2925753	-130.3176503
OBH	-100.5598755	-100.5431995	-100.5422555	-100.5652865
HON	-130.1370196	-100.4732179	-100.4722739	-100.4972209

[a] Energies in hartrees.

Table 10: [B, N, O, H_2] Relative Energies, Enthalpies, Free Energies[a].

STRUCTURE	E0+ZPE	H 298	G 298
NH_2BO, 1'	0.0	0.0	0.0
HOBNH, 2'	85.14340525	86.58215733	84.48704025
HBONH, 3'	331.2991836	329.5558781	331.4724639
HONBH, 4'	417.9926604	418.6280217	418.2604573
***bent*-HONBH, 5'**	439.9097379	438.8858085	439.4240278
BH_2NO, 6'	444.250936	444.2588124	445.6818117
NH_2OB, 7'	494.7855276	495.0953319	492.7980544
HN(B)OH, 8'	572.7097055	572.9092404	571.2105678
HNOBH, 9'	580.337717	582.4643396	578.106076
OBH···NH, 10'	615.0841048	620.7603493	606.5277306
BH_2ON, 11'	626.1015851	626.5557897	626.8970995
OH_2NB, 12'	770.0770857	771.2664191	767.0210503
BOH···NH, 13'	779.5912276	784.2304155	769.7326253
HNO–BH, 14'	840.2333151	842.664491	835.1031662
OH_2BN, 15'	846.6011058	847.3152309	845.4248997

[a] Relative QCISD(T)/aug-cc-pVTZ//QCISD/aug-cc-pVDZ energies in kJ/mol.

Table 11: [B, N, O, H_2] Fragmentation Energies.

Fragmentations	ΔE (kJ/mol)
10' → OBH + NH	2.404396268
13' → BOH + NH	22.66822164
14' → HNO + BH	20.63979124
4' → HON + BH	523.4925698
5' → HON + BH	503.8050329
9' → HNO + BH	294.5264657
3' → HNO + BH	553.2739502

Table 12: [B, N, O, H_2] MP2 and QCISD Frequencies (cm^{-1}) and Intensities (km/mol).

Structure	MP2 Frequencies[a]	QCISD Frequencies[a]
[NH_2BO], 1', C_s	a' 249.4 (212.4), a" 399.6 (9.2), a' 500.8 (26.9), a' 962.7 (3.8), a" 970.8 (20.1), a' 1586.1 (1.7), a' 1986.6 (342.4), a' 3624.8 (71.0), a" 3738.1 (79.2)	a' 250.5 (212.4), a" 403.2 (11.3), a' 505.9 (33.6), a' 966.5 (3.1), a" 980.4 (20.9), a' 1602.4 (34.7), a' 2004.0 (374.6), a' 3620.7 (59.1), a" 3725.1 (64.9)
[HOBNH], 2', C_s	a" 123.8 (129.4), a' 312.2 (95.5), a' 454.4 (33.6), a" 483.7 (1.0), a' 965.7 (80.8), a' 1012.4 (92.1), a' 2024.2 (399.7), a' 3861.6 (183.9), a' 3886.9 (209.5)	a" 125.3 (141.0), a' 324.2 (100.6), a' 456.4 (33.0), a" 486.9 (0.12), a' 973.3 (62.3), a' 1029.2 (110.1), a' 2044.7 (423.9), a' 3882.6 (185.2), a' 3896.5 (171.0)
[*c*-HBONH], 3', C_1	a 597.6 (19.8), a 740.0 (34.6), a 833.4 (9.11), a 969.3 (52.4), a 1066.0 (101.5), a 1193.9 (3.4), a 1356.2 (56.5), a 2803.0 (58.3), a 3451.2 (9.0)	a 584.2 (26.2), a 736.5 (34.6), a 831.5 (6.0), a 978.0 (55.8), a 1046.8 (68.6), a 1209.4 (6.5), a 1369.4 (56.5), a 2771.8 (58.2), a 3447.7 (5.7)
[HONBH], 4', C_s	a' 220.6 (16.6), a" 267.6 (32.8), a" 619.8 (0.038), a' 664.5 (1.4), a' 971.6 (44.1), a' 1399.7 (61.4), a' 1936.7 (0.67), a' 2907.8 (2.0), a' 3754.4 (85.5)	a' 204.4 (18.0), a" 261.2 (37.1), a" 630.2 (0.071), a' 674.8 (2.4), a' 975.8 (40.1), a' 1426.0 (57.7), a' 1967.5 (1.9), a' 2873.0 (6.6), a' 3782.7 (66.8)
[*bent*-HONBH], 5', C_1	a 511.6 (12.4), a 701.8 (32.8), a 750.5 (30.5), a 841.9 (42.3), a 872.0 (55.8), a 1150.7 (39.4) a 1530.0 (13.3), a 2841.0 (24.5), a 3729.2 (112.0)	a 370.9 (9.9), a 653.2 (60.0), a 784.2 (31.7), a 816.5 (18.9), a 930.3 (61.6), a 1105.0 (53.4), a 1463.7 (17.1), a 2782.9 (40.2), a 3789.4 (100.9)
[BH_2NO], 6', C_{2v}	b_1 295.9 (11.2), b_2 324.8 (1.3), b_1 790.7 (0.18), b_2 831.8 (5.9), a_1 964.9 (2.3), a_1 1170.1 (5.3), a_1 1884.7 (199.2), a_1 2630.9 (1.0), b_2 2746.2 (22.2)	b_1 237.6 (2.2), b_2 333.7 (1.8), b_1 780.4 (0.41), b_2 836.6 (6.3), a_1 963.4 (2.8), a_1 1157.1 (9.0), a_1 1926.9 (240.2), a_1 2607.7 (1.8), b_2 2717.4 (24.9)
[NH_2OB], 7', C_s	a' 163.9 (0.51), a" 234.2 (31.3), a' 822.4 (9.1), a' 1141.6 (124.7), a" 1310.8 (2.1), a' 1320.7 (163.7), a' 1617.3 (46.0), a' 3468.0 (2.8), a" 3579.7 (17.7)	a" 204.9 (32.6), a' 205.1 (1.3), a' 846.8 (10.2), a' 1146.3 (140.1), a' 1328.1 (179.4), a" 1332.3 (2.6), a' 1636.3 (45.3), a' 3454.1 (1.0), a" 3550.5 (9.0)
[HN(B)OH], 8', C_1	a 268.4 (44.5), a 289.2 (35.6), a 505.4 (150.4), a 934.8 (43.6), a 1189.4 (15.6), a 1382.0 (31.8), a 1438.4 (144.2), a 3578.6 (48.5), a 3760.0 (57.5)	a 274.4 (59.7), a 299.2 (14.1), a 501.7 (153.9), a 946.6 (49.2), a 1191.6 (22.1), a 1402.9 (32.0), a 1446.9 (130.0), a 3579.1 (36.3), a 3783.0 (46.3)

[HNOBH], 9', C_s	a' 229.9 (5.7), a" 330.8 (37.2), a' 460.9 (82.2), a" 568.7 (1.1), a' 706.1 (12.6), a' 1443.5 (27.7), a' 1727.4 (10.9), a' 2915.5 (11.9), a' 3422.3 (14.6)	a' 153.9 (13.3), a' 220.5 (0.15), a" 236.0 (55.8), a" 669.8 (7.1), a' 738.6 (14.1), a' 1329.8 (16.5), a' 1761.3 (29.2), a' 2875.4 (0.021), a' 3366.6 (23.9)
[OBH···NH], 10', $C_{\infty v}$	π 71.7 (0.86), π 73.0 (2.3), σ 88.5 (0.35), π 110.9 (121.6), π 217.1 (105.3), π 806.5 (9.2), π 818.4 (8.1), σ 1755.1 (55.6), σ 2900.6 (1.5), σ 3394.7 (6.6)	π 70.5 (2.2), π 73.0 (3.5), σ 86.7 (0.32), π 125.4 (113.0), π 206.3 (101.0), π 807.1 (10.5), π 815.9 (9.8), σ 1783.4 (76.3), σ 2867.1 (.043), σ 3323.2 (15.3)
[BH_2ON], 11', C_{2v}	b_1 222.6 (0.73), b_2 245.4 (0.55), b_1 911.4 (13.4), a_1 922.3 (46.4), b_2 949.5 (36.0), a_1 1210.1 (35.9), a_1 1546.9 (30.1), a_1 2666.6 (40.1), b_2 2805.1 (67.6)	b_1 207.9 (1.1), b_2 218.2 (0.18), b_1 846.4 (6.9), a_1 911.7 (16.4), b_2 931.0 (33.5), a_1 1172.4 (6.2), a_1 1504.6 (69.2), a_1 2626.7 (27.3), b_2 2757.1 (64.7)
[OH_2NB], 12', C_s	a" 157.2 (45.8), a' 285.6 (38.7), a' 664.8 (105.1), a' 894.3 (161.6), a" 949.0 (1.1), a' 1292.1 (133.9), a' 1601.4 (101.6), a' 3670.8 (171.5), a" 3780.4 (224.0)	a" 160.8 (49.1), a' 251.7 (9.7), a' 426.4 (131.7), a' 821.7 (200.1), a" 847.8 (1.3), a' 1217.5 (98.0), a' 1627.0 (87.3), a' 3734.4 (167.2), a" 3834.6 (183.1)
[BOH···NH], 13', C_s	a" 70.7 (95.3), a' 119.8 (31.7), a' 224.1 (24.7), a' 353.2 (51.1), a" 500.6 (152.5), a' 910.1 (165.4), a' 1400.0 (158.6), a' 3255.2 (1630.3), a' 3384.1 (2.13)	a" 58.9 (82.7), a' 109.9 (26.0), a' 191.6 (17.5), a' 298.3 (49.8), a" 450.1 (139.4), a' 854.3 (163.5), a' 1368.6 (181.3), a' 3322.2 (1.3), a' 3524.8 (1119.0)
[HNO—BH], 14', C_s	a" 97.6 (23.0), a' 227.4 (56.9), a' 344.5 (94.4), a" 690.9 (95.2), a' 860.0 (15.5), a' 1474.2 (14.1), a' 1582.9 (117.7), a' 2457.1 (322.5), a' 2959.5 (82.6)	a' 151.9 (45.4), a" 159.0 (20.5), a' 273.8 (64.4), a" 541.7 (95.5), a' 733.8 (4.0), a' 1552.4 (29.4), a' 1623.7 (88.0), a' 2385.6 (343.0), a' 2992.5 (31.3)
[OH_2BN], 15', C_s	a" 200.5 (0.42), a' 224.5 (25.7), a' 637.6 (84.9), a' 702.5 (135.8), a" 934.1 (5.9), a' 1622.2 (111.2), a' 1772.3 (4.5), a' 3675.8 (163.6), a" 3777.6 (305.3)	a" 197.9 (0.31), a' 235.5 (23.0), a' 645.5 (83.0), a' 702.5 (139.8), a" 941.9 (5.4), a' 1644.5 (108.7), a' 1889.2 (18.6), a' 3699.7 (117.9), a" 3791.4 (268.9)

[a] IR intensities in parentheses.

Table 13: Observed IR frequencies[a] for reaction of B_n + NO (in cm^{-1}).

Observed IR Absorptions	Assignment
897.4	NBO asymmetric stretch
1997.4	BO stretch, OBNNO
1627.4	NO stretch, OBNNO
2029.9	BO stretch, OBON
1148.6	NO stretch, OBON
2068.8	BO stretch, BNBO
1965.4	BO stretch, $BNBO^-$
1943.0	NO stretch, BBNO
1859.5	NO stretch, BBBNO

[a] Reference 1.

Figure 1: [B, H_2, C, F] Structures and Relative Energies. Atom color scheme: H: turquoise, C: black, B: yellow, F: green.

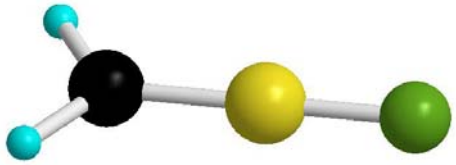

H_2CBF, **1**, C_{2v} 0 kJ/mol

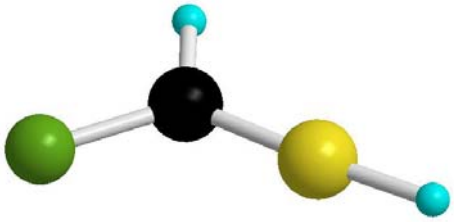

FCHBH, **2**, C_s
246.5 kJ/mol

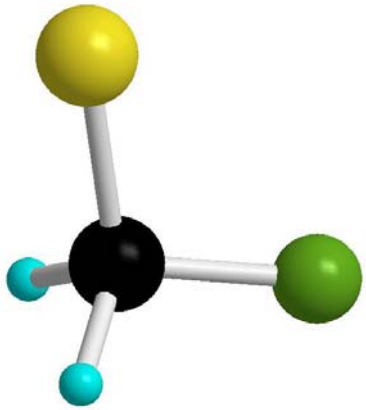

H_2CBF, **3**, C_s
348.6 kJ/mol

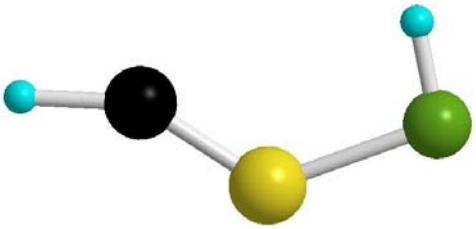

HCBFH, **5**, C_s
494.0 kJ/mol

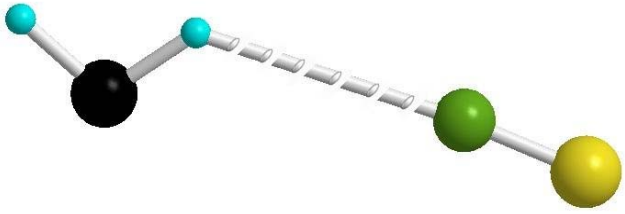

HCH···FB, **4**, C_s
463.9 kJ/mol

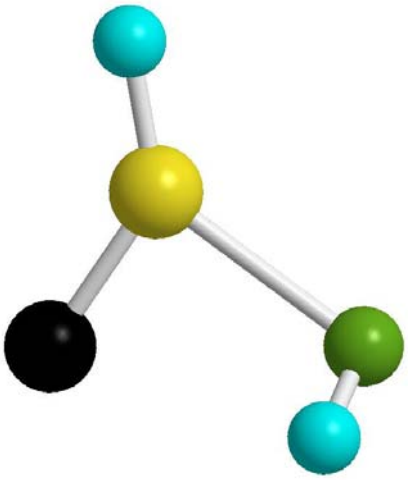

CBHFH, **6**, C_1
593.7 kJ/mol

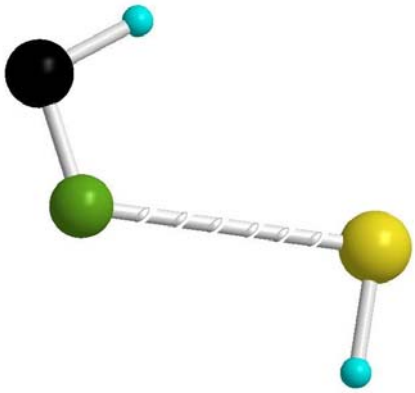

HCF─BH, **7**, C_s
721.7 kJ/mol

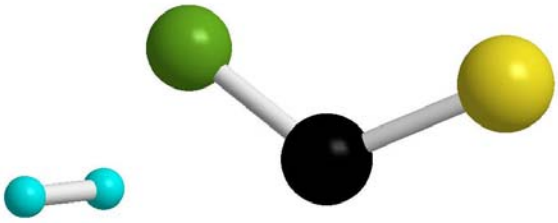

HH····C(F)B, **8**, C_1
761.9 kJ/mol

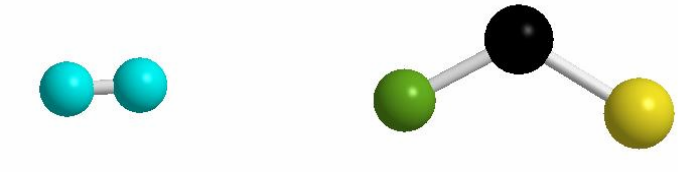

HH····FCB, **9**, C_1

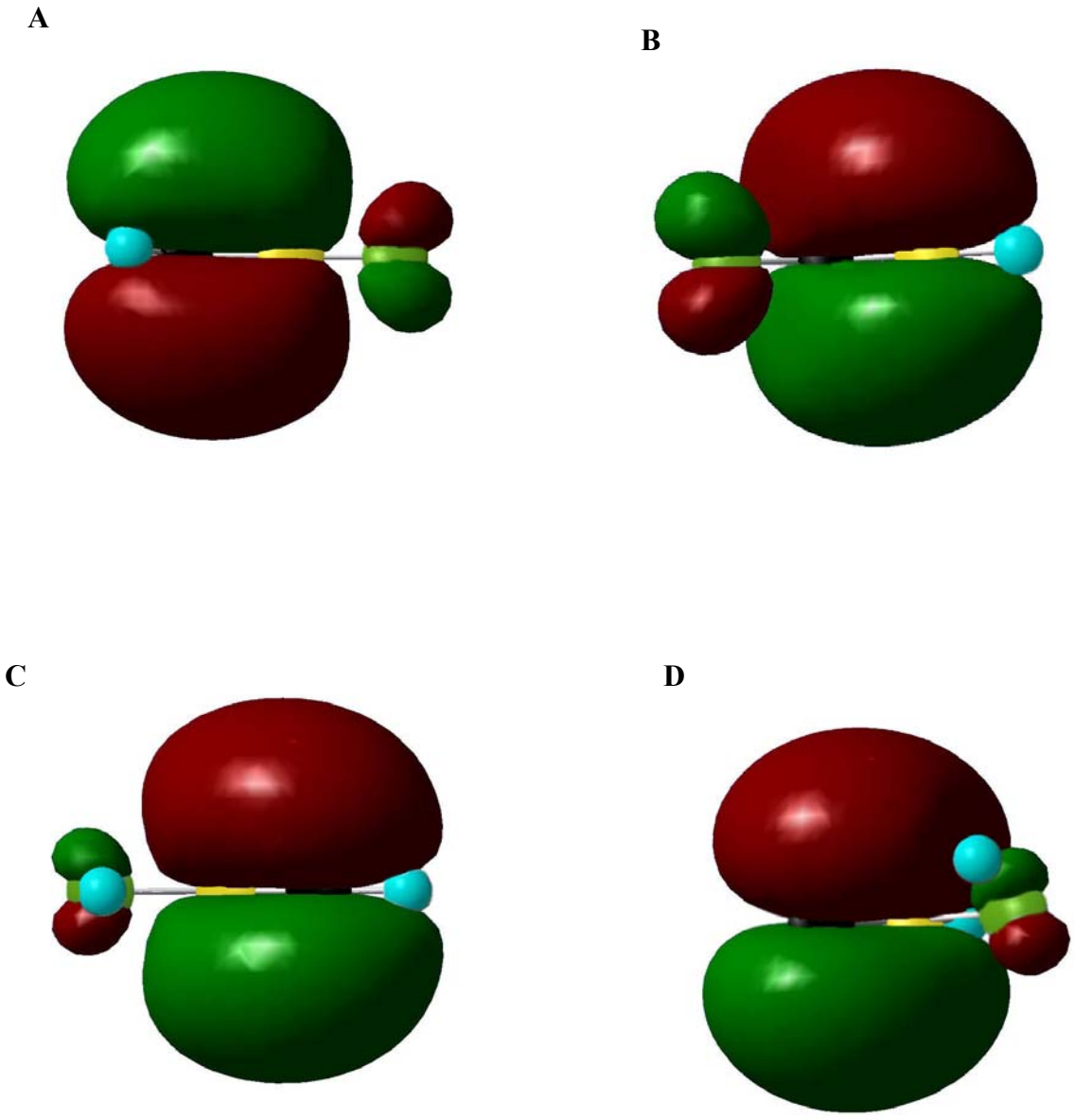

Figure 2: Delocalized Molecular Orbital Diagrams Showing CB Multiple Bond Character for **1** (A), **2** (B), **5** (C) and **6** (D). Atom color scheme: H: turquoise, C: black, B: yellow, F: green.

Figure 3: Transition Structures and Connected Minima. Atom color scheme: H: turquoise, C: black, B: yellow, F: green.

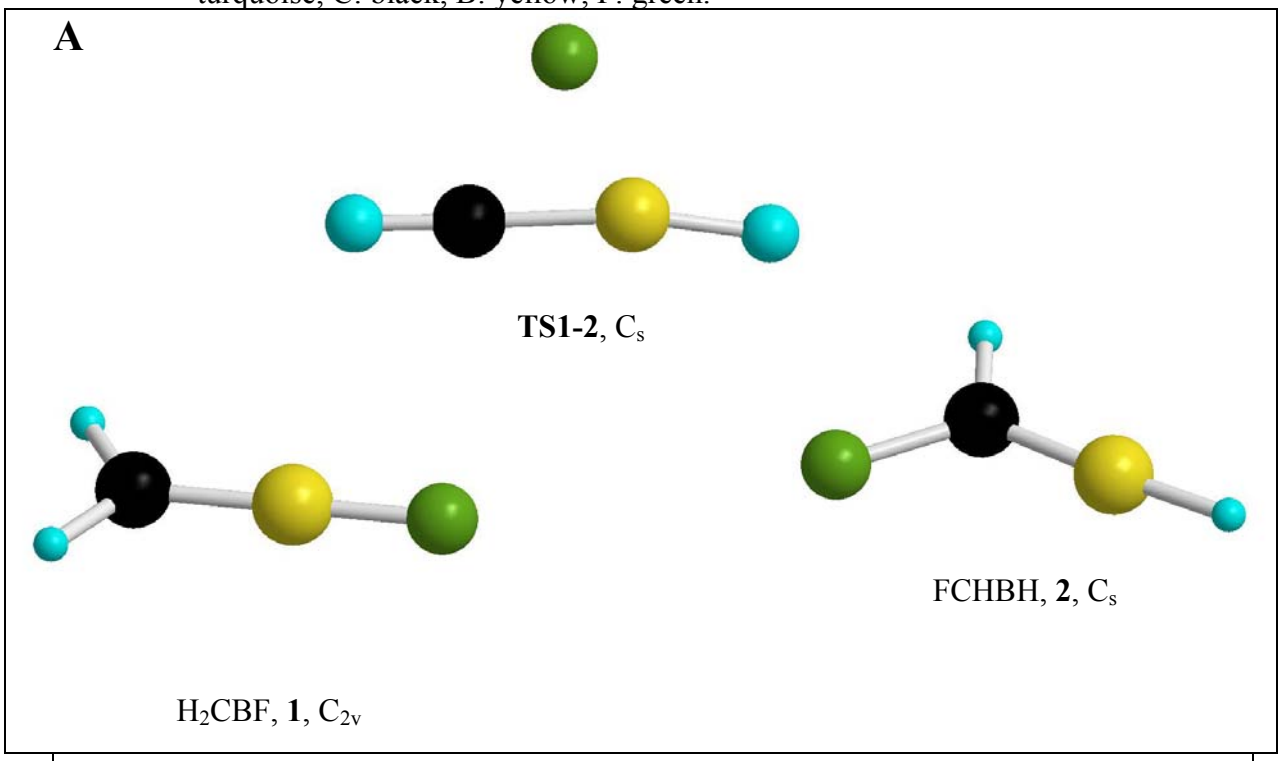

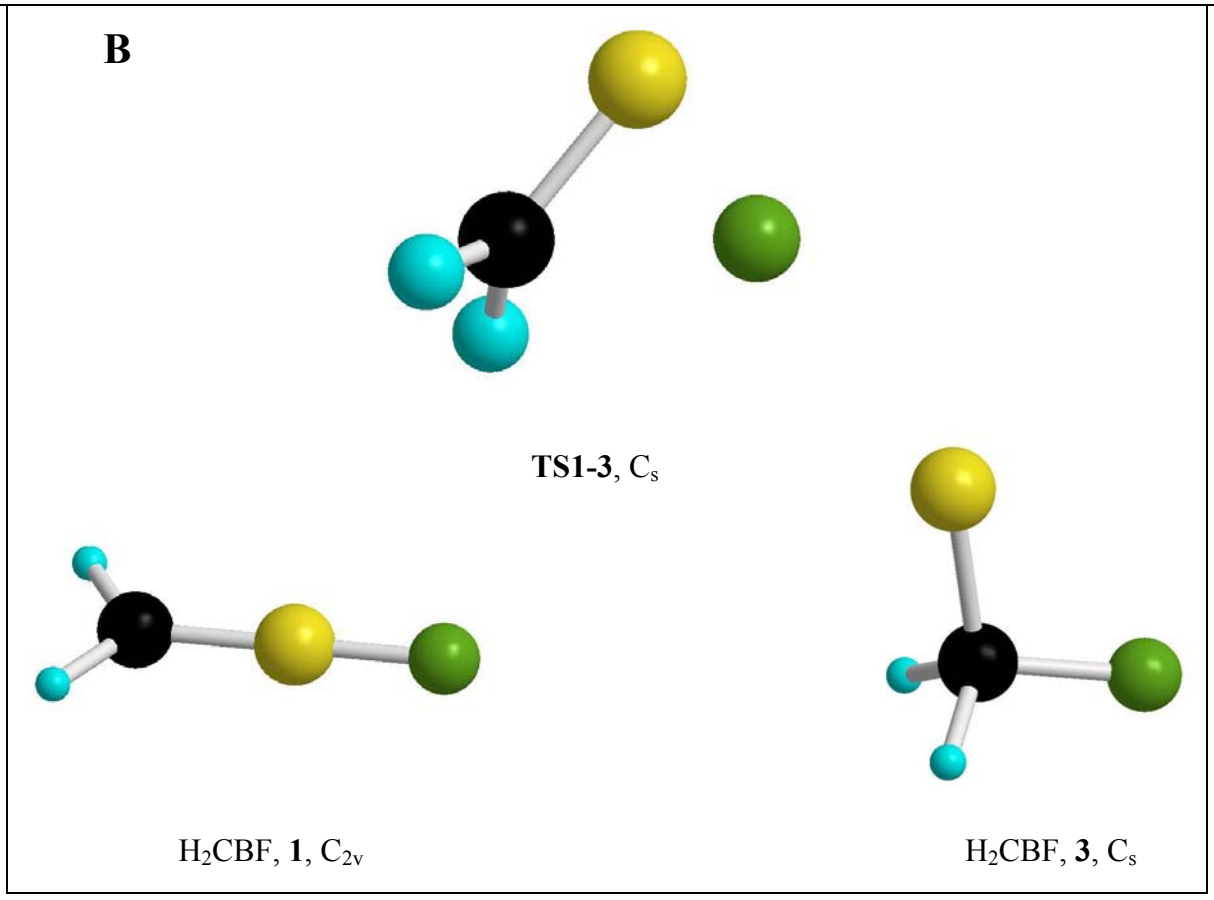

C

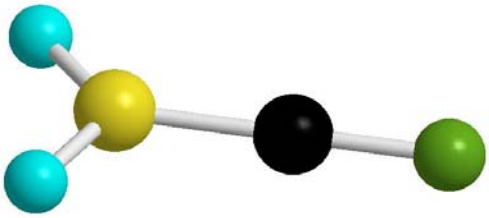

TS2-2, C_s

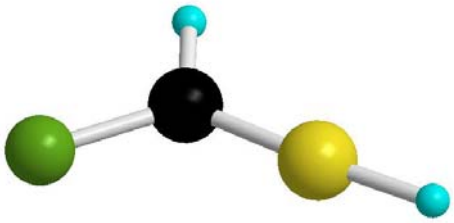

FCHBH, **2**, C_s

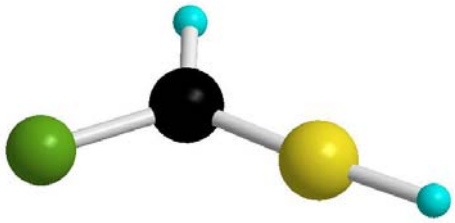

FCHBH, **2**, C_s

D

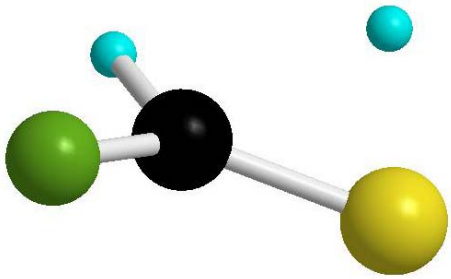

TS2-3, C_1

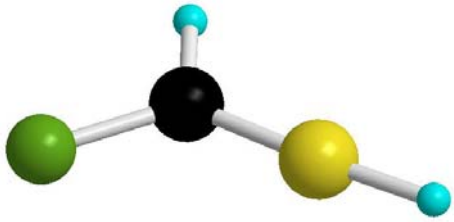

FCHBH, **2**, C_s

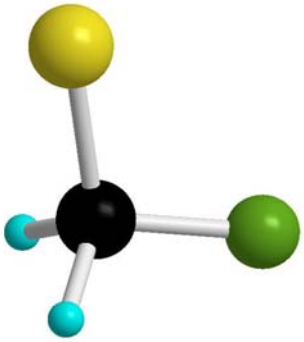

H_2CBF, **3**, C_s

E

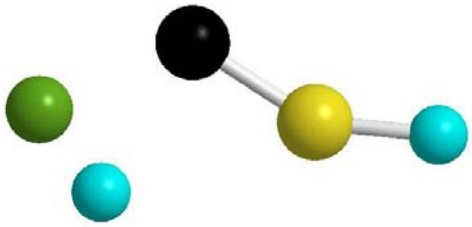

TS2-5, C_1

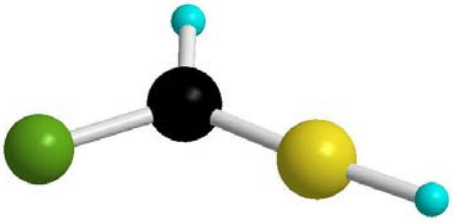

FCHBH, **2**, C_s

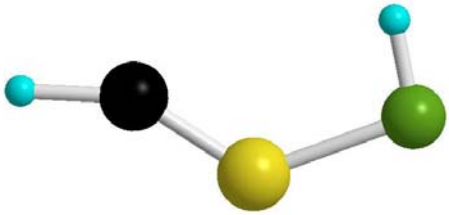

HCBFH, **5**, C_s

F

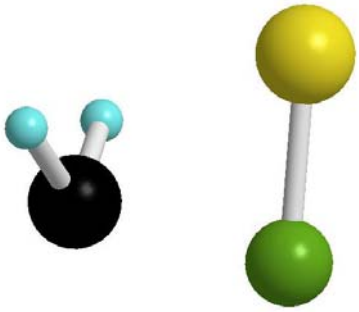

TS3-4, C_s

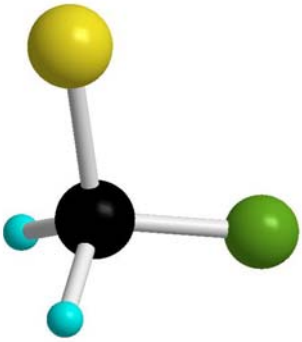

H_2CBF, **3**, C_s

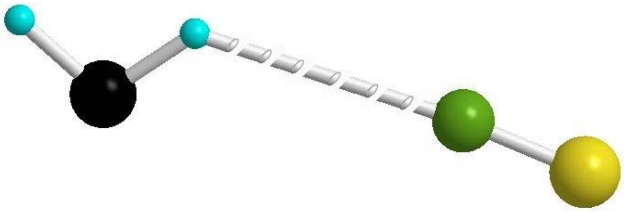

HCH···FB, **4**, C_1

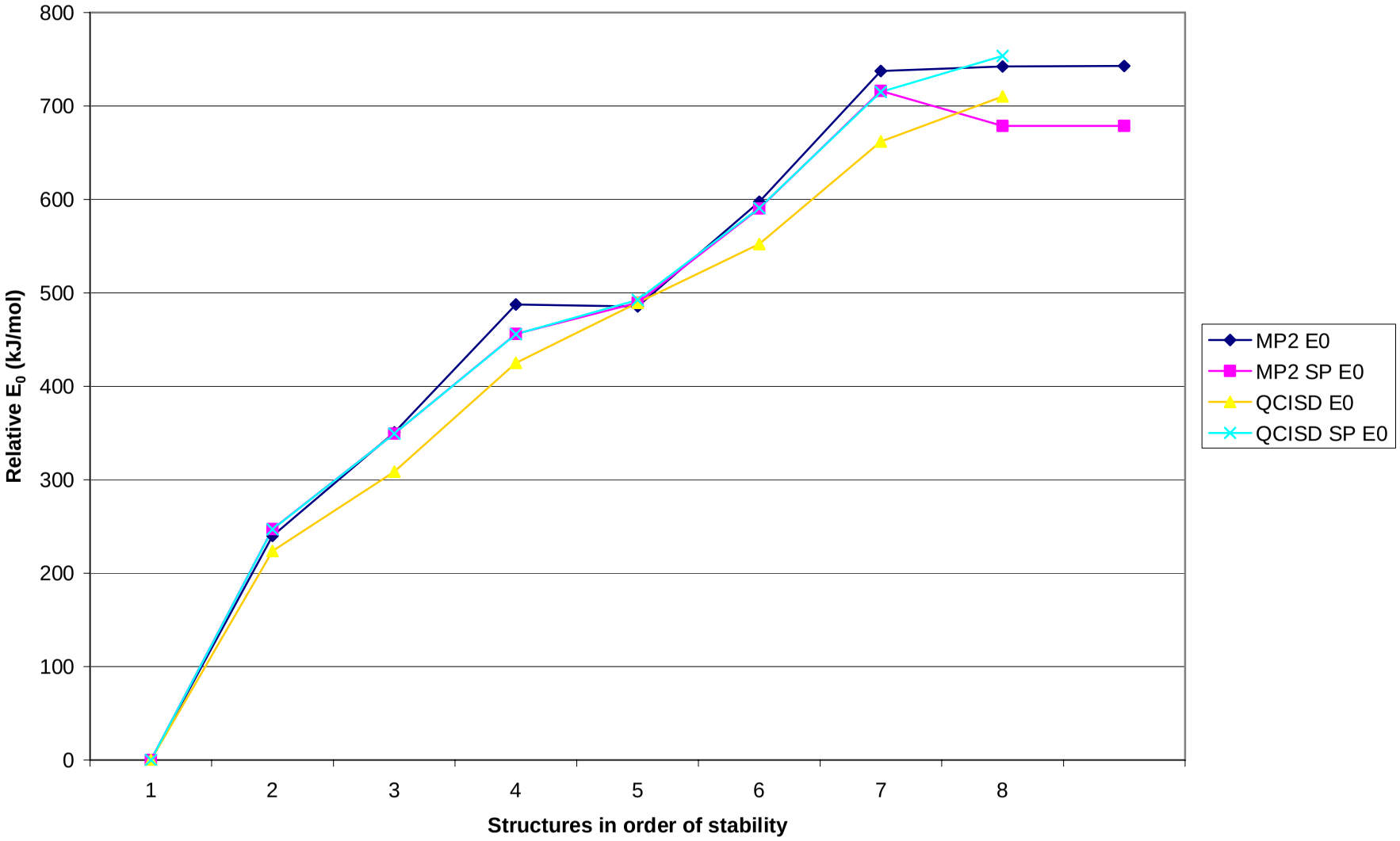

Figure 4: [B, C, F, H_2] Comparison of E_0 for the Four Computational Levels.

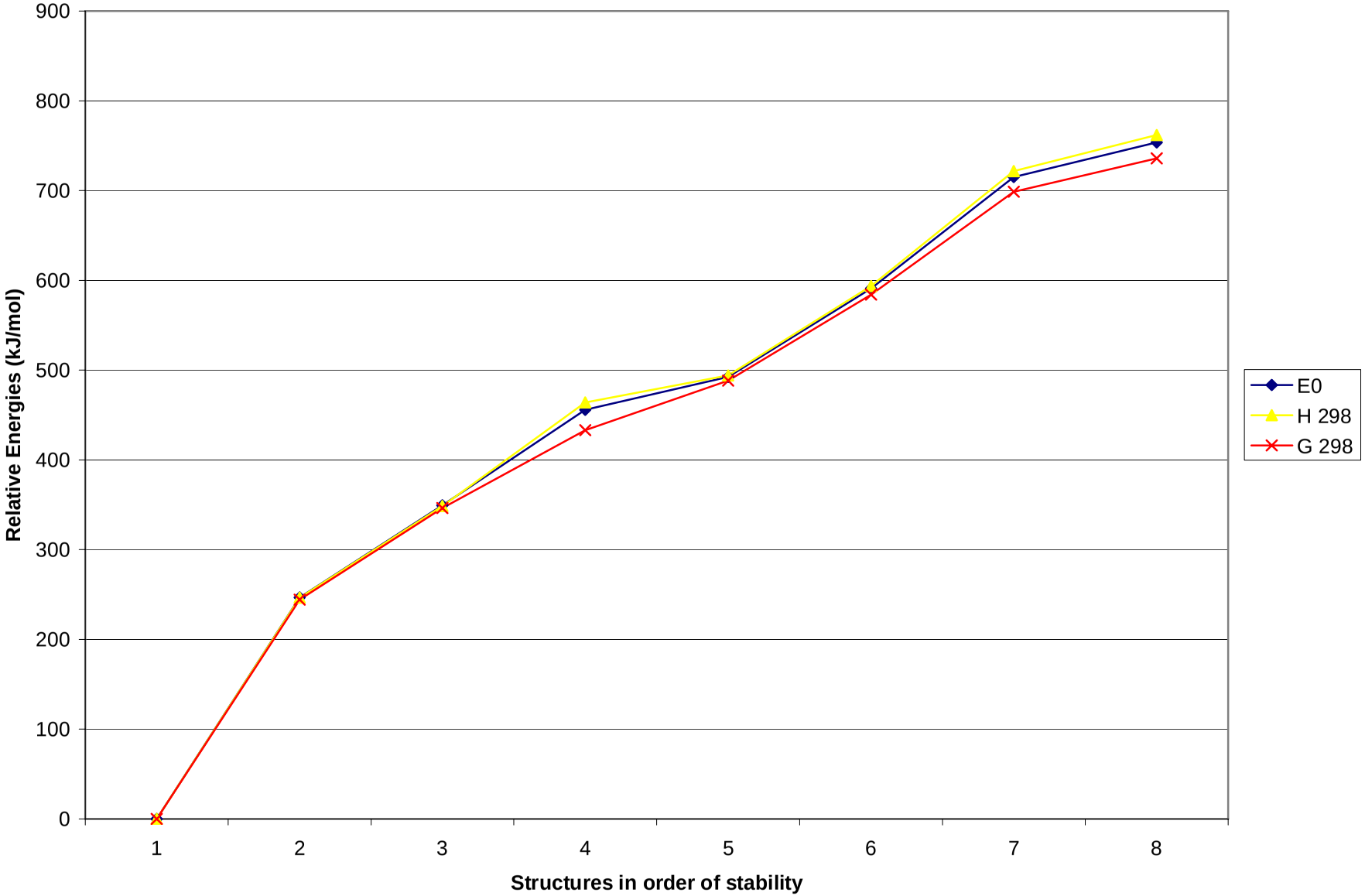

Figure 5: Comparison of QCISD(T)/aug-cc-pVTZ//QCISD/aug-cc-pVDZ Thermochemical Data.

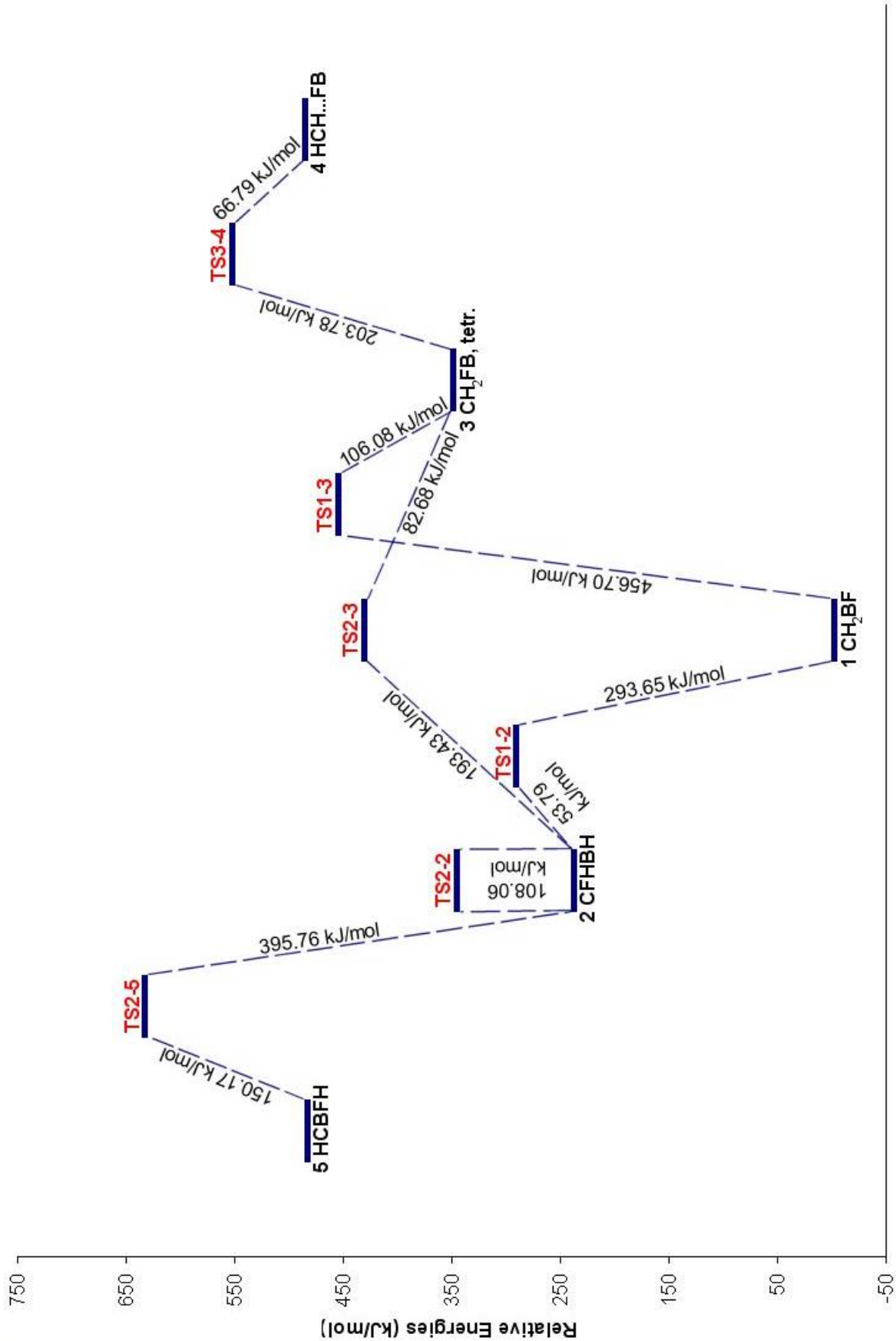

Figure 6: [B, C, F, H_2] Reaction Profile.

Figure 7: Protonations of [B, C, F H_2] Isomers (unstarred) to Form Corresponding [B, C, F, H_3]$^+$ Isomer(s) (starred). Atom color scheme: H: turquoise, C: black, B: yellow, F: green.

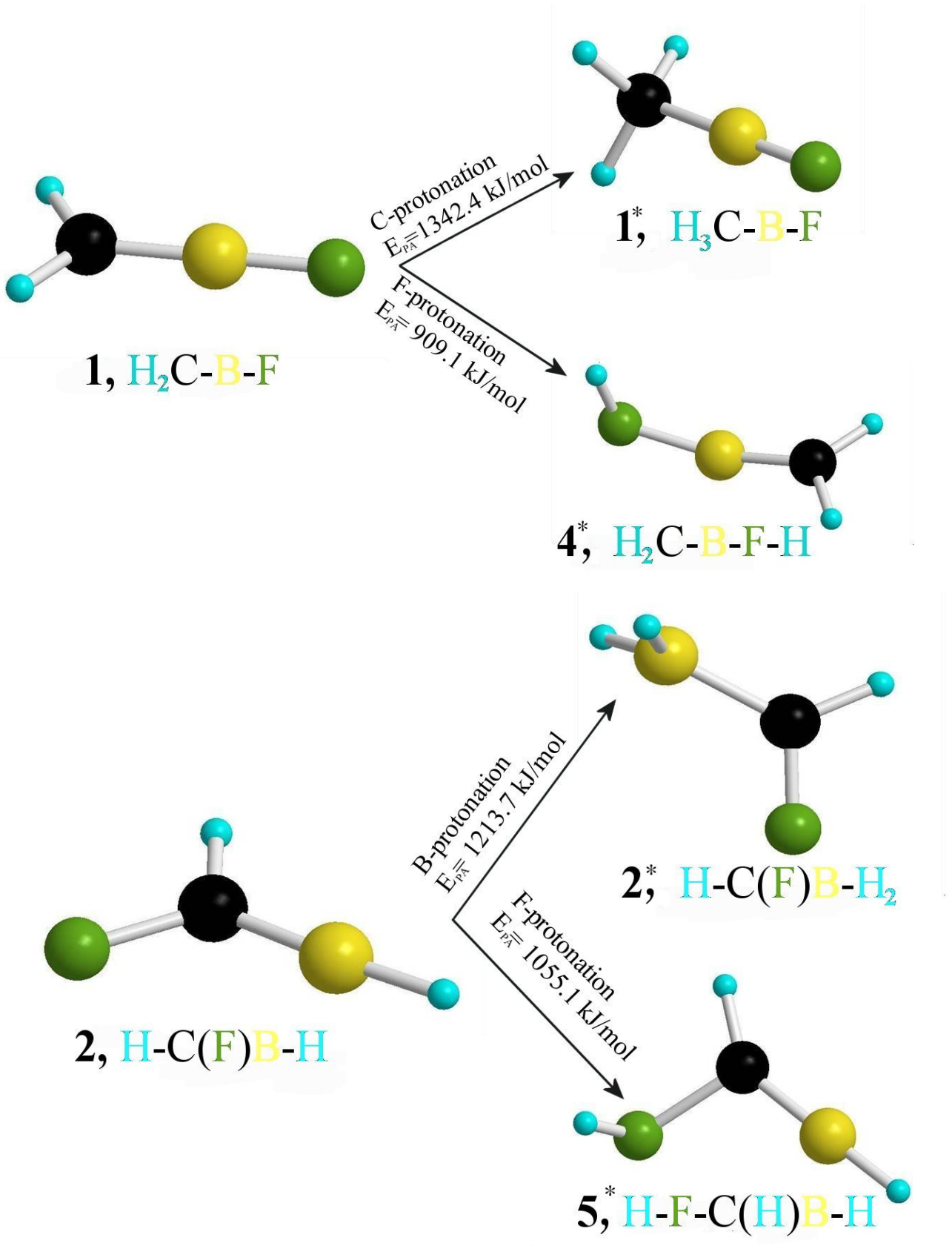

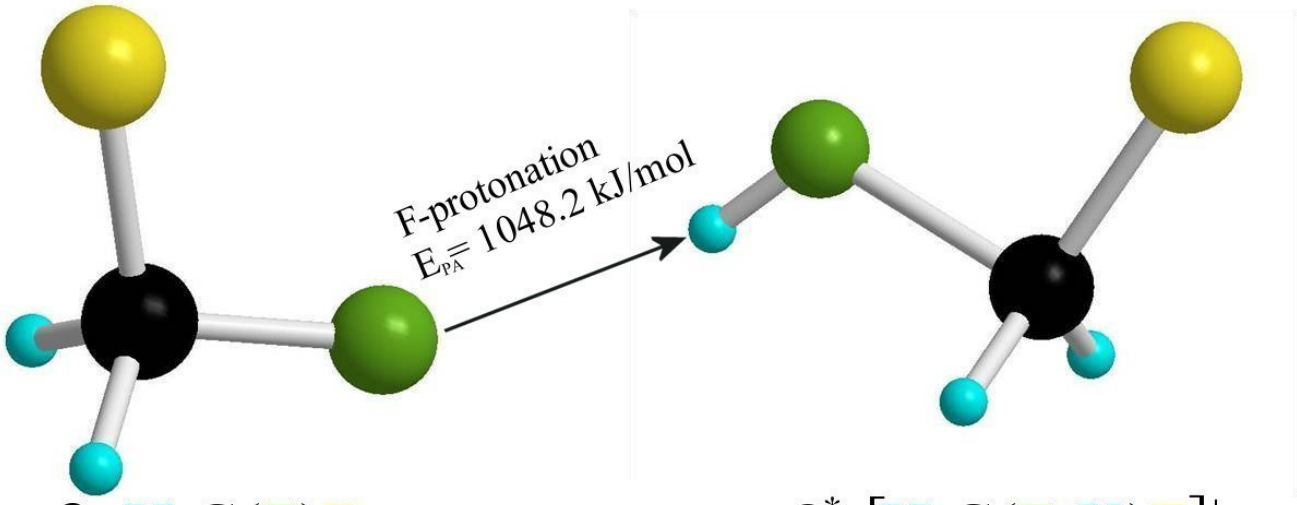

3, $H_2C(F)B$ **8*,** $[H_2C(F\text{-}H)B]^+$

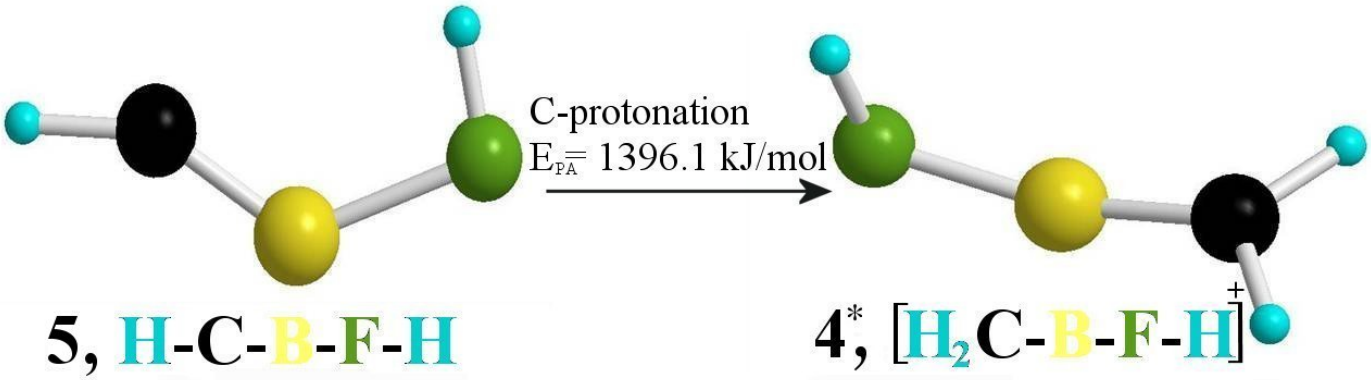

5, H-C-B-F-H **4*,** $[H_2C\text{-}B\text{-}F\text{-}H]^+$

Figure 8: [B, H_2, N, O] Structures and Relative Energies. Atom color scheme: H: turquoise, N: blue, B: yellow, O: red.

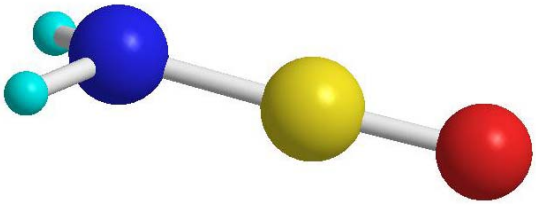

NH_2BO, **1'**, C_s 0 kJ/mol

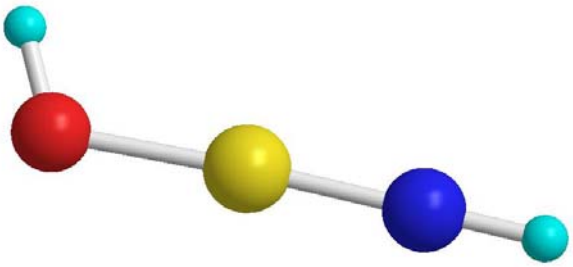

HOBNH, **2'**, C_s
86.58 kJ/mol

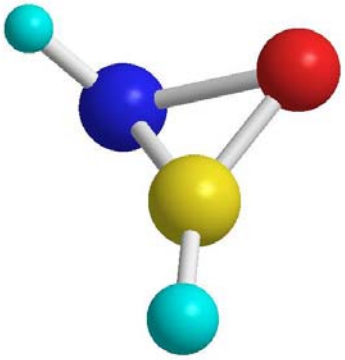

c-HBONH, **3',** C_1
329.6 kJ/mol

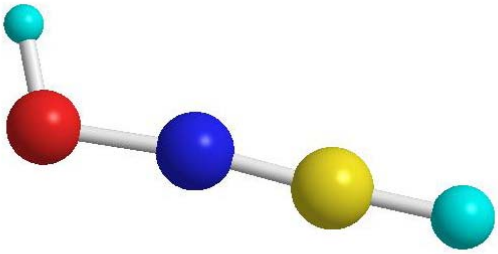

HONBH, **4'**, C_s
418.6 kJ/mol

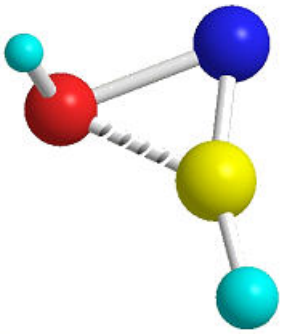

bent-HONBH, **5'**, C_1
438.9 kJ/mol

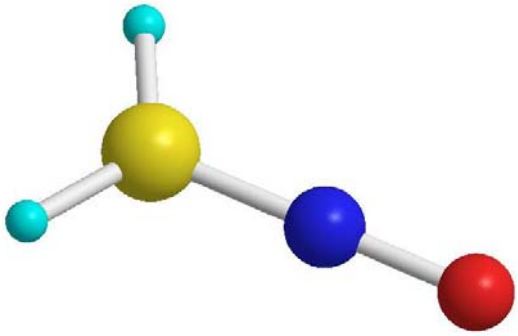

BH_2NO, **6'**, C_{2v}
444.3 kJ/mol

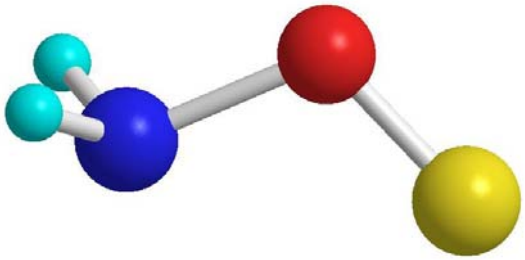

NH_2OB, **7'**, C_s
495.1 kJ/mol

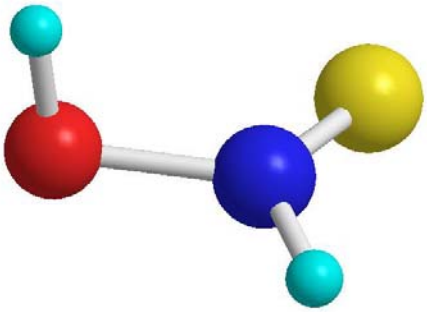

HON(H)B, **8'**, C_1
572.9 kJ/mol

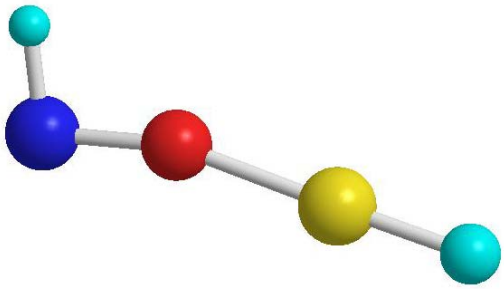

HNOBH, **9'**, C_s 582.5
kJ/mol

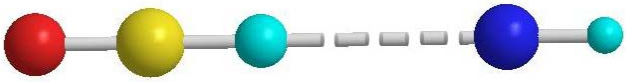

OBH…NH, **10'**, $C_{\infty v}$
620.8 kJ/mol

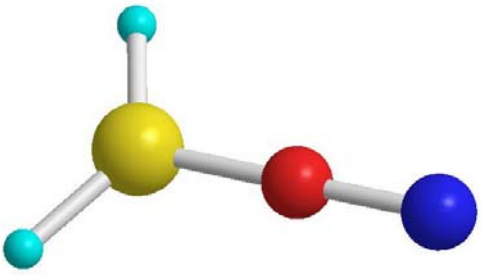

BH_2ON, **11'**, C_{2v}
626.6 kJ/mol

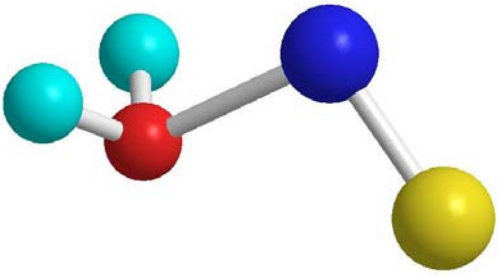

OH_2NB, **12'**, C_s
771.3 kJ/mol

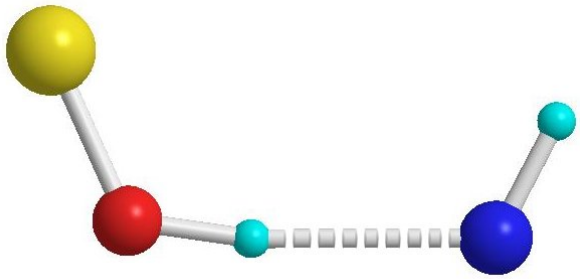

BOH···NH, **13'**, C_s
784.2 kJ/mol

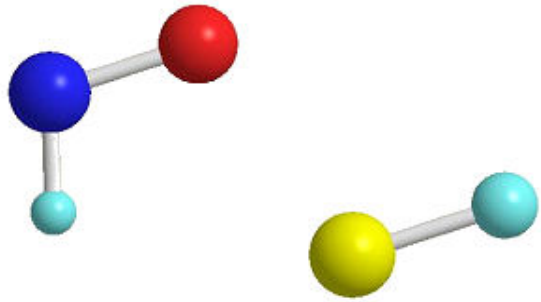

HNO–BH, **14'**, C_s
842.7 kJ/mol

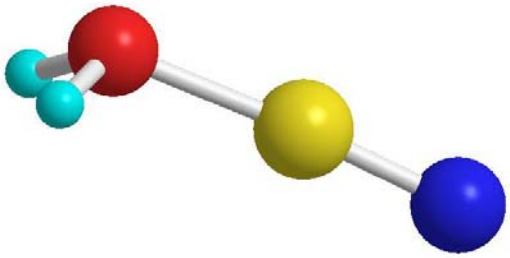

OH_2BN, **15'**, C_s
847.3 kJ/mol

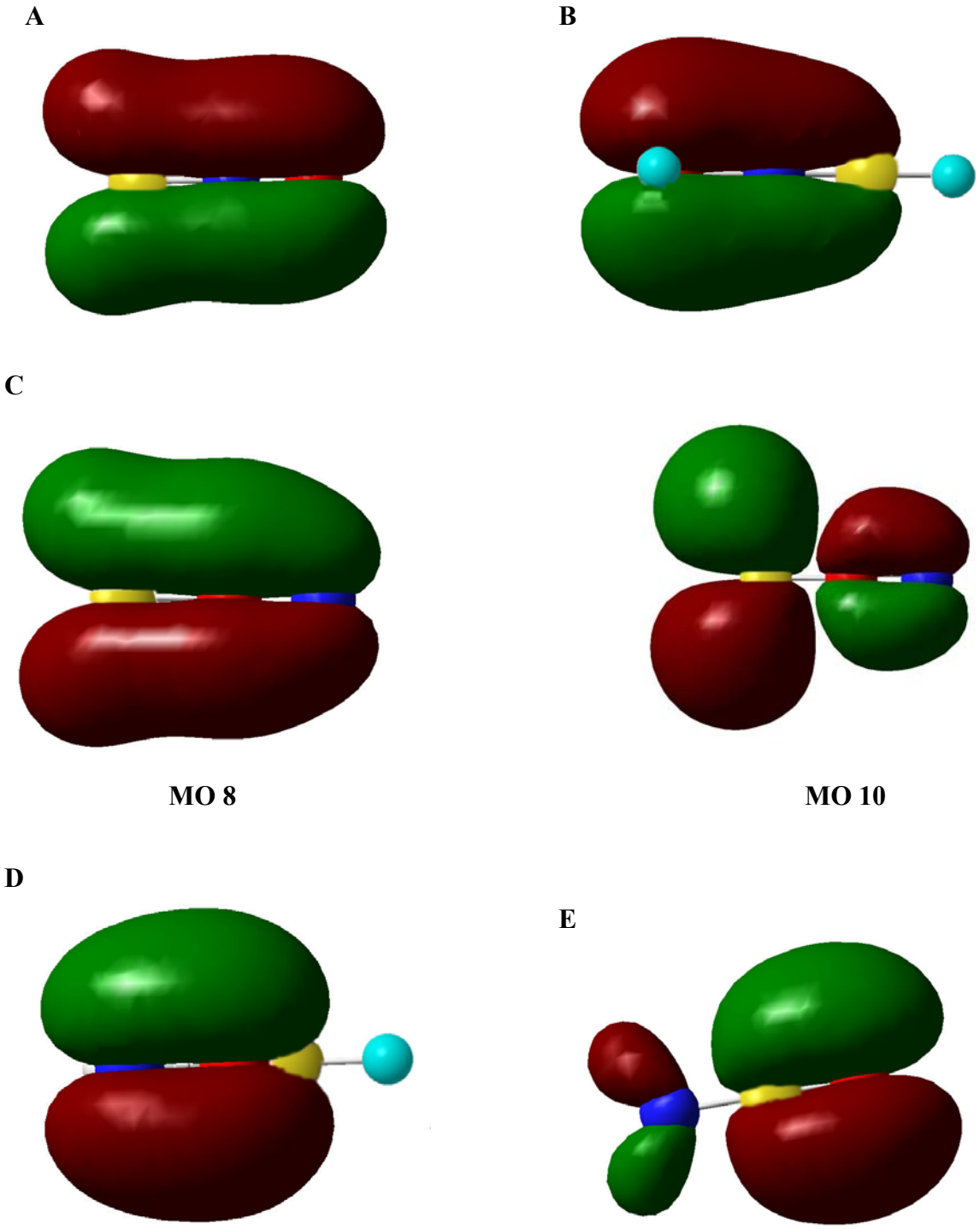

Figure 9: Delocalized Molecular Orbital Pictures For Multiple Bonding in **6'** (A), **4'** (B), **11'** (C), **14'** (D) and **1'** (E). Atom color scheme: H: turquoise, N: blue, B: yellow, O: red.

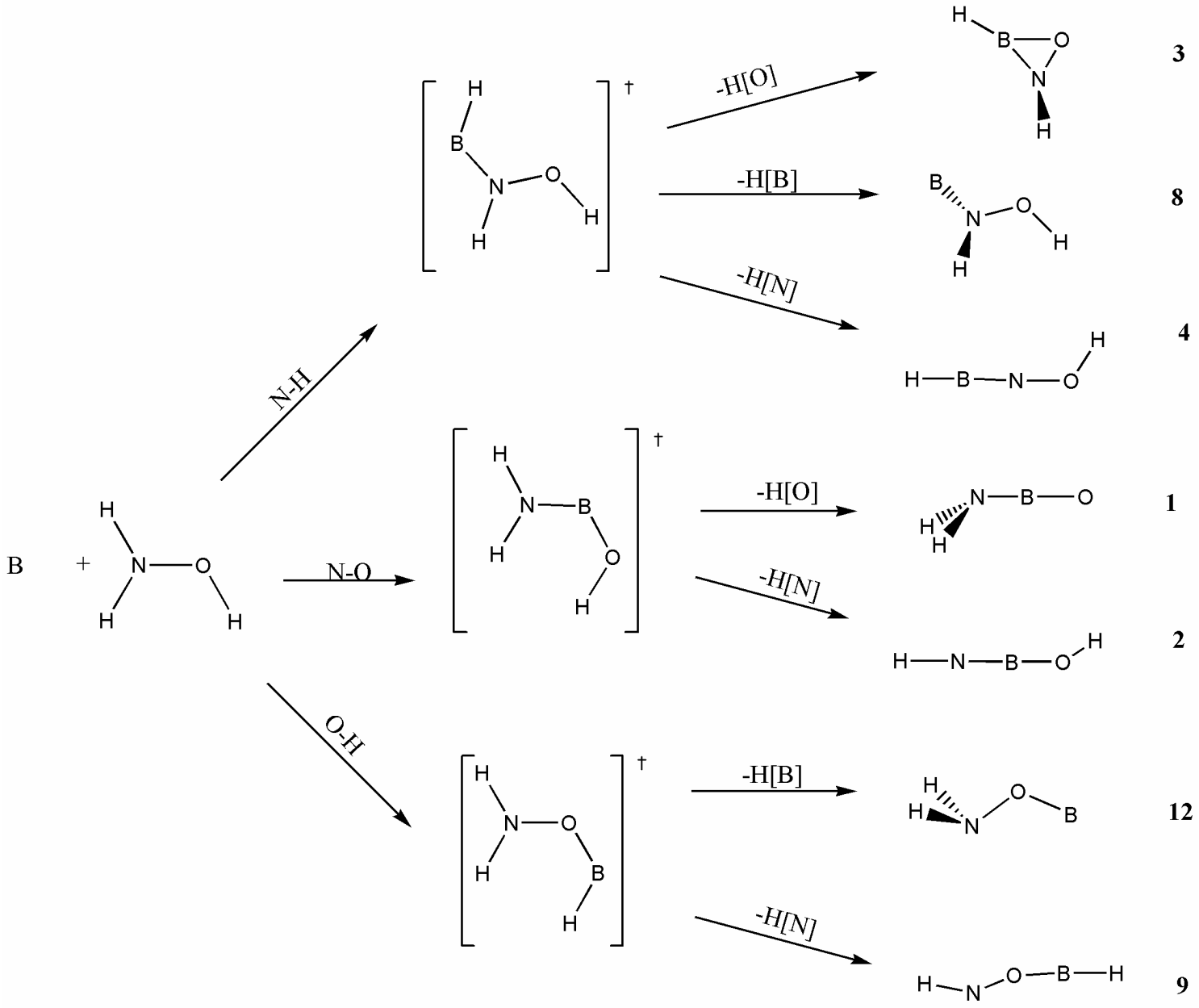

Figure 10: B + H_2NOH Insertion Reactions.

REFERENCES

1. Zhou, M.; Tsumori, N.; Xu, Q.; Kushto, G. P.; Andrews, L. *J. Am. Chem. Soc.* **2003,** *125,* 11371.
2. Lanzisera, D. V.; Andrews, L. *J. Phys. Chem. A* **1997**, *101*, 824.
3. Lanzisera, D. V.; Andrews L. *J. Phys. Chem. A* **2000**, *104*, 9295.
4. Lanzisera, D.V.; Andrews, L. *J. Phys. Chem. A* **1997**, *101*, 1482.
5. Andrews, L; Lanzisera, D. V.; Hassanzadeh, P.; Hannachi, Y. *J. Phys. Chem. A* **1998**, *102*, 3259.
6. Lanzisera, D.V.; Andrews, L. *J. Phys. Chem. A*, **1997**, *101*, 7134.
7. Hassanzadeh, P.; Andrews, L. *J. Am. Chem. Soc.* **1992,** *114,* 9239.
8. Hassanzadeh, P.; Hannachi, Y.; Andrews, L. *J. Phys. Chem.* **1993***, 97,* 6418.
9. Thompson, C. A.; Andrews, L. *J. Am. Chem. Soc.* **1995**, *117*, 10125.
10. Thompson, C. A.; Andrews, L.; Martin, J. M. L.; El-Yazal, J. *J. Phys. Chem.* **1995**, *99*, 13839.
11. DiMare, M. *J. Org. Chem.* **1996**, *61*, 8378.
12. Brown, H. C.; Schlesinger, H. I.; Burg, A. B. *J. Am. Chem. Soc.* **1939**, *61*, 673.
13. Rozas, I.; Alkorta, I.; Elguero, J. *J. Phys. Chem. A* **1999**, *103*, 8861.
14. Schuurman, M. S.; Allen, W. D.; Schleyer, P. von R.; Schaefer, H. F. *J. Chem. Phys.* **2005**, *122*, 104302.
15. Tague, T. J.; Andrews, L. *J. Am. Chem. Soc.* **1994**, *116*, 4970.
16. Ford, T. A. *Spectrochim. Acta Part A*, **2005**, *61*, 1403.
17. Kiani, F. A.; Hofmann, M. *Inorg. Chem.* **2004**, *43*, 8561.
18. Malde, A.; Khedkar, S.; Coutinho, E,; Saran, A. *Int. J. of Quantum Chem.* **2005**, *102*, 734.
19. Jacquemin, D.; Medved, M.; Perpète, E. A. *Int. J. Quantum Chem.* **2005**, *103*, 226.
20. Páppova, A.; Deakyne, C. A.; Skancke, A.; Černušák, I.; Liebman, J. F. *Mol. Phys.* **1996**, *89*, 247.
21. Deakyne, C. A.; Li, L.; Liebman, J. F. *Int. J. Mass Spec.* **2003**, *227*, 555.
22. Deakyne, C. A. *Int. J. Mass Spec.* **2003**, *227*, 601.

23. Gaussian 98, Revision A.11.3, M. J. Frisch, G. W. Trucks, H. B. Schlegel, G. E. Scuseria, M. A. Robb, J. R. Cheeseman, V. G. Zakrzewski, J. A. Montgomery, Jr., R. E. Stratmann, J. C. Burant, S. Dapprich, J. M. Millam, A. D. Daniels, K. N. Kudin, M. C. Strain, O. Farkas, J. Tomasi, V. Barone, M. Cossi, R. Cammi, B. Mennucci, C. Pomelli, C. Adamo, S. Clifford, J. Ochterski, G. A. Petersson, P. Y. Ayala, Q. Cui, K. Morokuma, N. Rega, P. Salvador, J. J. Dannenberg, D. K. Malick, A. D. Rabuck, K. Raghavachari, J. B. Foresman, J. Cioslowski, J. V. Ortiz, A. G. Baboul, B. B. Stefanov, G. Liu, A. Liashenko, P. Piskorz, I. Komaromi, R. Gomperts, R. L. Martin, D. J. Fox, T. Keith, M. A. Al-Laham, C. Y. Peng, A. Nanayakkara, M. Challacombe, P. M. W. Gill, B. Johnson, W. Chen, M. W. Wong, J. L. Andres, C. Gonzalez, M. Head-Gordon, E. S. Replogle, and J. A. Pople, Gaussian, Inc., Pittsburgh PA, 2002.

24. Gaussian 03, Revision B.04, M. J. Frisch, G. W. Trucks, H. B. Schlegel, G. E. Scuseria, M. A. Robb, J. R. Cheeseman, J. A. Montgomery, Jr., T. Vreven, K. N. Kudin, J. C. Burant, J. M. Millam, S. S. Iyengar, J. Tomasi, V. Barone, B. Mennucci, M. Cossi, G. Scalmani, N. Rega, G. A. Petersson, H. Nakatsuji, M. Hada, M. Ehara, K. Toyota, R. Fukuda, J. Hasegawa, M. Ishida, T. Nakajima, Y. Honda, O. Kitao, H. Nakai, M. Klene, X. Li, J. E. Knox, H. P. Hratchian, J. B. Cross, V. Bakken, C. Adamo, J. Jaramillo, R. Gomperts, R. E. Stratmann, O. Yazyev, A. J. Austin, R. Cammi, C. Pomelli, J. W. Ochterski, P. Y. Ayala, K. Morokuma, G. A. Voth, P. Salvador, J. J. Dannenberg, V. G. Zakrzewski, S. Dapprich, A. D. Daniels, M. C. Strain, O. Farkas, D. K. Malick, A. D. Rabuck, K. Raghavachari, J. B. Foresman, J. V. Ortiz, Q. Cui, A. G. Baboul, S. Clifford, J. Cioslowski, B. B. Stefanov, G. Liu, A. Liashenko, P. Piskorz, I. Komaromi, R. L. Martin, D. J. Fox, T. Keith, M. A. Al-Laham, C. Y. Peng, A. Nanayakkara, M. Challacombe, P. M. W. Gill, B. Johnson, W. Chen, M. W. Wong, C. Gonzalez, and J. A. Pople, Gaussian, Inc., Wallingford CT, 2004.

25. Møller, C.; Plesset, M. S. *Phys. Rev.* **1934**, *46*, 618.

26. Pople, J. A.; Binkley, J. S.; Seeger, R. *Int. J. Quantum Chem. Sym.* **1976**, *10*, 110.

27. Pople, J. A.; Head-Gordon, M.; Raghavachari, K. *J. Chem. Phys.* **1987**, *87*, 5968.

28. Dunning, T. H., Jr. *J. Chem. Phys.* **1989**, *90*, 1007.

29. Woon, D. E.; Dunning, T. H., Jr. *J. Chem. Phys.* **1993**, *98*, 1358.

30. Peng, C.; Schlegel, H. B. *Israel J. Chem.,* **1993**, *33*, 449.

31. Peng, C.; Ayala, P. Y.; Schlegel, H. B.; Frisch, M. J. *J. Comp. Chem.*, **1995**, *16*, 49.

32. Gonzalez, C.; Schlegel, H. B. *J. Chem. Phys.* **1989**, *90,* 2154.

33. Gonzalez, C.; Schlegel, H. B. *J. Phys. Chem.* **1990**, *94,* 5523.

34. Jensen, F. *Introduction to Computational Chemistry*; John Wiley & Sons: New York, 1999; p 162.

35. Jensen, F. *Introduction to Computational Chemistry*; John Wiley & Sons: New York, 1999; p 98.

36. Jensen, F. *Introduction to Computational Chemistry*; John Wiley & Sons: New York, 1999; p 101.

37. Cizek, J. *J. Chem. Phys.* **1966**, *45*, 4256.

38. Cramer, C. J. *Essentials of Computational Chemistry: Theories and Models;* John Wiley & Sons: West Sussex, UK, 2002; pp 211-213.

39. NBO Version 3.1, E.D. Glendening, A. E. Reed, J. E. Carpenter, and F. Weinhold.

40. Bader, R.F.W. *Atoms in Molecules: A Quantum Theory;* Oxford University Press: Oxford, UK, 1990.

41. Carpenter, J. E.; Weinhold, F. *J. Mol. Struct. (Theochem)* **1988**, *169*, 41.

42. Carpenter, J. E. PhD thesis, University of Wisconsin, Madison, WI, 1987.

43. Foster, J. P.; Weinhold, F. *J. Amer. Chem. Soc.* **1980**, *102*, 7211.

44. Reed, A. E.; Weinhold, F. *J. Chem. Phys.* **1983**, *78,* 4066.

45. Reed, A. E.; Weinstock, R. B.; Weinhold, F. *J. Chem. Phys.* **1985**, *83*, 735.

46. Reed, A. E.; Curtiss, L. A.; Weinhold, F. *Chem. Rev.* **1988**, *88*, 899.

47. Weinhold, F.; Carpenter, J. E. *Plenum* **1988**, 227.

48. Popelier, P. *Atoms in Molecules, An Introduction.* Prentice Hall: New York, NY, 2000, p 2.

49. van Duijneveldt, F. B.; van Duijneveldt-van de Rijdt, J. G. C. M.; van Lenthe, J. H. *Chem. Rev.* **1997**, *94*, 1873.

50. Alabugin, I. V.; Manoharan, M.; Peabody, S.; Weinhold, F. *J. Am. Chem. Soc.* **2003**, *125,* 5973.

51. Becker, C.; Kieltsch, I.; Broggini, D.; Mezzetti, A; *Inorg. Chem.* **2003**, *42*, 8417.

52. Mezzetti, A.; Becker, C. *Helv. Chim. Acta*, **2002**, *85*, 2686.

53. Katz, H. E. *J. Org. Chem.* **1985**, *50*, 5027.

54. Wang, H.; Webster, C. E.; Pérez, L. M.; Hall, M. B.; Gabbaï, F. P. *J. Am. Chem. Soc.* **2004**, *126*, 8189.

55. Solé, S.; Gabbaï, F. P. *Coord. Chem. Rev.* **2002**, *235*, 93.

56. Frisch, Æ.; Frisch, M. J. *Gaussian 98 User's Reference*; Gaussian, Inc.: Pittsburgh, PA, 1999, 2nd Edition, p 43.

57. Hammond, G. S. *J. Am. Chem. Soc.* **1955**, *77*, 334.

58. NIST Chemistry WebBook. http://webbook.nist.gov/chemistry/ (accessed 05/12/2005).

59. Li, X.; Liu, L; Schlegel, J. B. *J. Am. Chem. Soc.* **2002**, *365,* 464.

60. Zhang, L. N.; Zhou, M. F. *Chem. Phys.* **2000**, 256, 185.

61. Gurvich, L. V.; Veyts, I. V.; Alcock, C. B. *Thermodynamic Properties of Individual Substances*; 4th ed.; Hemisphere Publishing Company.: New York, NY, 1989.